



AFTAC

Air Force Technical Applications Center

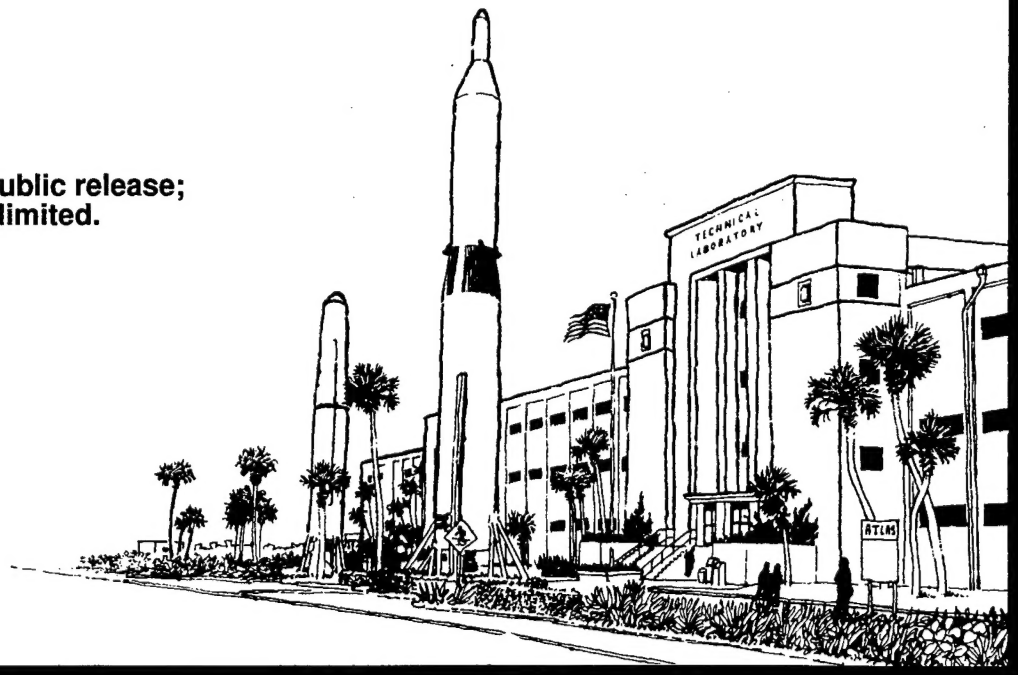
**NOISE POWER SPECTRAL DENSITY AND COHERENCY ESTIMATES AT SITES
IN NEVADA, USA: MINA, EXCELSIOR MOUNTAINS, GABBS VALLEYS,
GARFIELD (GAR) SEISMIC STATIONS, AND EAST OF GARFIELD**

**Bao V. Nguyen and David R. Russell
Directorate of Nuclear Treaty Monitoring
Research Division**

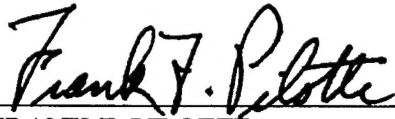
6 JULY 1998

19980921 088

**Approved for public release;
Distribution unlimited.**



Report AFTAC-TR-98-005 has been reviewed and is approved for publication.



FRANK F. PILOTTE

Director of Nuclear Treaty Monitoring



JOHN T. WIGINGTON III

Colonel, USAF

Commander

Addressees: Please notify HQ AFTAC/TTR, 1030 S. Highway A1A, Patrick Air Force Base FL 32925-3002, if there is a change in your mailing address (including an individual no longer employed by your organization) or if your organization no longer wishes to be included in the distribution of future reports of this nature.

REPORT DOCUMENTATION PAGE			Form Approved OMB No. 0704-0188	
Public reporting burden for this collection of information is estimated to average 1 hour per response, including the time for reviewing instructions, searching existing data sources, gathering and maintaining the data needed, and completing and reviewing the collection of information. Send comments regarding this burden estimate or any other aspect of this collection of information, including suggestions for reducing this burden, to Washington Headquarters Services, Directorate for Information Operations and Reports, 1215 Jefferson David Highway, Suite 1204, Arlington, VA 22202-4302, and to the Office of Management and Budget, Paperwork Reduction Project (0704-0188), Washington, DC 20503.				
1. AGENCY USE ONLY (Leave blank)		2. REPORT DATE 6 July 1998		3. REPORT TYPE AND DATES COVERED Technical
4. TITLE AND SUBTITLE Noise Power Spectral Density and Coherency Estimates at Sites in Nevada, USA: Mina, Excelsior Mountains, Gabbs Valleys, Garfield (GAR) Seismic Stations, and East of Garfield			5. FUNDING NUMBERS	
6. AUTHORS Bao V. Nguyen and David R. Russell				
7. PERFORMING ORGANIZATION NAME(S) AND ADDRESS(ES) HQ Air Force Technical Applications Center (HQ AFTAC/TTR) 1030 S. Highway A1A Patrick AFB FL 32925-3002			8. PERFORMING ORGANIZATION REPORT NUMBER AFTAC-TR-98-005	
9. SPONSORING/MONITORING AGENCY NAME(S) AND ADDRESS(ES)			10. SPONSORING/MONITORING AGENCY REPORT NUMBER	
11. SUPPLEMENTARY NOTES				
12a. DISTRIBUTION/AVAILABILITY STATEMENT Approved for public release; distribution unlimited.			12b. DISTRIBUTION CODE A	
13. ABSTRACT (Maximum 200 words) Noise was analyzed for displacement power spectral density (PSD) in decibels (dB) referenced to units of nanometers (nm) ² /Hertz (Hz) from noise time series acquired in 1997, days 216-224, in the state of Nevada, USA, at MINA seismic stations, GABBS Valleys, Excelsior Mountains, GAR seismic stations, and nearby to the east of GAR seismic stations. The noise surveys at MINA seismic stations and GABBS Valleys were conducted by the Allied-Signal Technical Services Corp. with four sites at each location. The noise survey to the east of GAR seismic stations composed of four sites and at the Excelsior Mountains near MINA composed of two sites were conducted by the Lawrence Livermore National Laboratory (LLNL). The Southern Methodist University (SMU) conducted the noise surveys at the existing locations of GAR seismic stations. AlliedSignal employed the Teledyne Geotech GS-13 seismometer and the RDAS-200P digitizer for their noise survey. The LLNL and the SMU used the GS-13 and the REFTEK digitizer. The PSD results at 1 Hz and 6 Hz are as follows: (Continued on next page)				
14. SUBJECT TERMS Mina Gabbs Valley Garfield Coherence Noise Power Spectral Density			15. NUMBER OF PAGES 49	
			16. PRICE CODE	
17. SECURITY CLASSIFICATION OF REPORT UNCLASSIFIED	18. SECURITY CLASSIFICATION OF THIS PAGE UNCLASSIFIED	19. SECURITY CLASSIFICATION OF ABSTRACT UNCLASSIFIED	20. LIMITATION OF ABSTRACT See Block 12a	

Block 13 Con't:

Name	Latitude (°)	Longitude (°)	Displacement Power Spectral Density in dB referred to 1 nm ² /Hz (Day/Night)	Standard Deviation (Day/ Night)	Noise RMS Amplitude (nm) (0.8-3.0 Hz)	Noise Surveyed By
			1 Hz	1 Hz		
			6 Hz	6 Hz		
MINA, Site 1	38.2758	-118.4710	-2.5/-9.0 -26.7/-32.7	5.4/5.8 6.3/7.6	0.62/0.33	AlliedSignal
MINA, Site 2	38.2796	-118.4740	-5.5/-9.2 -34.7/-40.1	4.3/4.3 11.1/7.5	0.45/0.31	AlliedSignal
MINA, Site 3	38.2736	-118.4660	-0.2/-6.8 -25.6/-32.0	6.2/6.2 8.2/9.7	0.82/0.41	AlliedSignal
MINA, Site 4	38.2735	-118.4750	-4.2/-9.5 -40.5/-45.3	5.3/5.3 6.5/6.5	0.53/0.27	AlliedSignal
GABBS, Site 1	38.6191	-118.2260	-7.2/-0.5 -40.1/-31.2	8.0/8.0 5.0/9.9	0.37/0.78	AlliedSignal
GABBS, Site 2	38.6192	-118.2300	-1.4/-8.5 -34.9/-38.5	4.7/4.7 5.2/5.7	0.72/0.33	AlliedSignal
GABBS, Site 3	38.6240	-118.2280	1.9/1.2 -34.9/-33.4	8.9/8.9 6.2/11.5	1.07/0.94	AlliedSignal
GABBS, Site 4	38.6179	-118.2200	-0.8/-5.9 -36.1/-35.8	6.8/4.3 5.3/6.4	0.77/0.42	AlliedSignal
LLNL, Site 1	38.4387	-118.2139	4.2/-8.2 -31.0/-36.5	8.6/12.4 9.7/14.1	0.51/0.32	LLNL
LLNL, Site 3	38.4208	-118.1900	-9.3/-12.9 -32.0/-37.4	9.9/14.5 9.6/14.8	0.33/0.21	LLNL
LLNL, Site 4	38.4150	-118.2106	-4.5/-5.0 -28.9/-30.7	4.7/4.0 6.4/4.8	0.51/0.48	LLNL
LLNL, Site 6	38.4336	-118.2193	-5.2/-5.7 -30.2/-32.3	4.6/4.2 6.2/5.3	0.54/0.52	LLNL
Excelsior Mountains, Site1	38.279	-118.4734	-2.3/-6.0 -33.9/-39.2	7.1/7.1 7.8/9.8	0.65/0.43	LLNL
Excelsior Mountains, Site2	38.2737	-118.4749	-7.4/-8.8 -39.1/-44.3	4.7/3.2 5.8/5.7	0.36/0.31	LLNL

Name	Latitude (°)	Longitude (°)	Displacement Power Spectral Density in dB referred to 1 nm ² /Hz (Day/Night)	Standard Deviation (Day/ Night)	Noise RMS Amplitude (nm) (0.8-3.0 Hz)	Noise Surveyed By
			1 Hz	1 Hz		
			6 Hz	6 Hz		
GARA0	38.4268	-118.3000	-8.8/-8.9 -31.0/-33.0	3.7/4.4 4.3/4.6	0.33/0.33	SMU
GARB1	38.4240	-118.3063	-9.6/-9.8 -30.2/-32.5	3.1/3.6 5.3/5.0	0.33/0.32	SMU
GARB2A	38.4208	-118.2898	-9.7/-11.1 -33.7/-37.6	2.3/1.8 7.1/2.0	0.28/0.25	SMU
GARB2	38.4258	-118.2908	-10.8/-11.2 -37.3/-39.3	3.3/3.6 3.8/3.9	0.26/0.25	SMU
GARB3	38.4342	-118.3043	-12.6/-12.3 -40.8/-42.3	2.5/3.0 3.8/3.9	0.21/0.21	SMU
GARBL1	38.4502	-118.2933	-13.5/-13.6 -44.1/-46.5	2.2/2.0 3.5/3.7	0.18/0.18	SMU
GARC4	38.4105	-118.2952	-8.8/-10.0 -35.1/-37.6	4.4/4.9 4.9/5.3	0.30/0.27	SMU

These results can be compared with the United States Geological Survey's (USGS's) New Low and High Noise Models (NLNM and NHHM) which give -18 and 32 dB re nm²/Hz at 1 Hz, respectively.

With respect to mean PSD values at 1 Hz, GABBS Valleys Site 3 is noisiest with daytime and nighttime noise at +1.9 and +1.2 dB, respectively. Furthermore, the noise levels at sites that are much quieter are LLNL Site 3 east of GAR seismic stations with daytime and nighttime noise levels at -9.3 and -12.9 dB, respectively; GARB3 with daytime and nighttime noise levels at -12.6 and -12.3 dB, respectively. The site at GARBL1 is the quietest site in this survey with daytime and nighttime noise levels at -13.5 and -13.6 dB, respectively.

With respect to mean PSD values at 6 Hz, daytime noise at MINA Site 3 is noisiest with a value of -25.6 dB. Furthermore, the noise levels at sites that are much quieter at night

are MINA Site 4 and LLNL Excelsior Mountains Site 2 with nighttime noise levels at -45.3 and -44.3 dB, respectively. The site at GARBL1 is the quietest site in this survey with daytime and nighttime noise levels at -44.1 and -46.5 dB, respectively.

Signal Coherence Spectra: Signal coherence is excellent with most of coherence values near unity at MINA up to about 2 Hz. Beyond 2 Hz, signal coherency is not interpretable. Good signal coherency is found for other sites such as GABBS, GAR, and LLNL sites. Signal coherency is representable and interpretable at these sites.

Noise Coherence Spectra: Noise coherency is good at GAR and LLNL sites; poorer noise coherency is at MINA and GABBS. Noise coherency is representable and interpretable at these sites.

CONTENTS

	Page
LIST OF FIGURES	vi
LIST OF TABLES	ix
ACKNOWLEDGMENTS	x
ABSTRACT	1
INTRODUCTION	4
PURPOSE	6
INSTRUMENT RESPONSES	6
NOISE ANALYSIS	8
COMPARISONS	10
COHERENCE ESTIMATES	15
DISCUSSIONS AND CONCLUSIONS	17
Noise Analysis	17
Coherence Analysis	18
REFERENCES	20
APPENDIX A: PLOTS OF DISPLACEMENT POWER SPECTRAL DENSITY	21
APPENDIX B: PLOTS OF SIGNAL AND NOISE COHERENCE SPECTRA.....	43
DISTRIBUTION	49

LIST OF FIGURES

FIGURE #	PAGE
1. Site locations of noise survey in Nevada, USA, days 216-224, year 1997.	4
2. The normalized velocity and displacement amplitude system responses for the GS13/RDAS-200P and GS13/REFTEK, respectively.	7
3a. Map of noise survey days 216-224 year 1997-upper part-showing PSD values (Day/Night) in dB (re nm ² /Hz) at 1 Hz and 6 Hz, respectively.	11
3b. Map of noise survey days 216-224 year 1997-middle part-showing PSD values (Day/Night) in dB (re nm ² /Hz) at 1 Hz and 6 Hz, respectively.	12
3c. Map of noise survey days 216-224 year 1997-lower part-showing PSD values (Day/Night) in dB (re nm ² /Hz) at 1 Hz and 6 Hz, respectively.	13
4. A composite of mean noise levels (day and night) at 1 Hz and 6 Hz for all the sites of this noise survey.	19
A1. Daytime mean noise PSD at Mina Site 1.	22
A2. Nighttime mean noise PSD at Mina Site 1.	22
A3. Daytime mean noise PSD at Mina Site 2.	23
A4. Nighttime mean noise PSD at Mina Site 2.	23
A5. Daytime mean noise PSD at Mina Site 3.	24
A6. Nighttime mean noise PSD at Mina Site 3.	24
A7. Daytime mean noise PSD at Mina Site 4.	25
A8. Nighttime mean noise PSD at Mina Site 4.	25
A9. Daytime mean noise PSD at Gabbs Site 1.	26
A10. Nighttime mean noise PSD at Gabbs Site 1.	26
A11. Daytime mean noise PSD at Gabbs Site 2.	27
A12. Nighttime mean noise PSD at Gabbs Site 2.	27
A13. Daytime mean noise PSD at Gabbs Site 3.	28

FIGURE #	PAGE
A14. Nighttime mean noise PSD at Gabbs Site 3.	28
A15. Daytime mean noise PSD at Gabbs Site 4.	29
A16. Nighttime mean noise PSD at Gabbs Site 4.	29
A17. Daytime mean noise PSD at LLNL Site 1 (east of GAR).	30
A18. Nighttime mean noise PSD at LLNL Site 1 (east of GAR).	30
A19. Daytime mean noise PSD at LLNL Site 3 (east of GAR).	31
A20. Nighttime mean noise PSD at LLNL Site 3 (east of GAR).	31
A21. Daytime mean noise PSD at LLNL Site 4 (east of GAR).	32
A22. Nighttime mean noise PSD at LLNL Site 4 (east of GAR).	32
A23. Daytime mean noise PSD at LLNL Site 6 (east of GAR).	33
A24. Nighttime mean noise PSD at LLNL Site 6 (east of GAR).	33
A25. Daytime mean noise PSD at LLNL Excelsior Mountains Site 1.	34
A26. Nighttime mean noise PSD at LLNL Excelsior Mountains Site 1.	34
A27. Daytime mean noise PSD at LLNL Excelsior Mountains Site 2.	35
A28. Nighttime mean noise PSD at LLNL Excelsior Mountains Site 2.	35
A29. Daytime mean noise PSD at SMU GARA0 seismic station.	36
A30. Nighttime mean noise PSD at SMU GARA0 seismic station.	36
A31. Daytime mean noise PSD at SMU GARB1 seismic station.	37
A32. Nighttime mean noise PSD at SMU GARB1 seismic station.	37
A33. Daytime mean noise PSD at SMU GARB2 seismic station.	38
A34. Nighttime mean noise PSD at SMU GARB2 seismic station.	38
A35. Daytime mean noise PSD at SMU GARB2A seismic station.	39
A36. Nighttime mean noise PSD at SMU GARB2A seismic station.	39

FIGURE #	PAGE
A37. Daytime mean noise PSD at SMU GARB3 seismic station.	40
A38. Nighttime mean noise PSD at SMU GARB3 seismic station.	40
A39. Daytime mean noise PSD at SMU GARBL1 seismic station.	41
A40. Nighttime mean noise PSD at SMU GARBL1 seismic station.	41
A41. Daytime mean noise PSD at SMU GARC4 seismic station.	42
A42. Nighttime mean noise PSD at SMU GARC4 seismic station.	42
B1. (a) Signals (P waves) recorded at MINA sites. (b) Signal correlation functions relative to site 4. (c) Pre-signal noise at four sites. (d) Noise correlation functions relative to site 4. (e-g) Signal and noise coherency of sites 1, 2, and 3, relative to site 4.	44
B2. Spectral multiplications for signals as well as for pre-signal noise of sites 1, 2, and 3, with site 4.	44
B3. (a) Signals (P waves) recorded at GABBS sites. (b) Signal correlation functions relative to site 2. (c) Pre-signal noise at three sites. (d) Noise correlation functions relative to site 2. (e-f) Signal and noise coherency of sites 1 and 4, relative to site 2.	45
B4. Spectral multiplications for signals as well as for pre-signal noise of sites 1 and 4, with site 2.	45
B5. (a) Signals (P waves) recorded at GAR sites. (b) Signal correlation functions relative to site B3. (c) Pre-signal noise at three sites. (d) Noise correlation functions relative to site B3. (e-f) Signal and noise coherency of sites BL1 and C4, relative to site B3.	46
B6. Spectral multiplications for signals as well as for pre-signal noise of sites BL1 and C4 with site B3.	46
B7. (a) Signals (P waves) recorded at LLNL sites. (b) Signal correlation functions relative to site 4. (c) Pre-signal noise at four sites. (d) Noise correlation functions relative to site 4. (e-g) Signal and noise coherency of sites 1, 3, and 6, relative to site 4.	47
B8. Spectral multiplications for signals as well as for pre-signal noise of sites 1, 3, and 6, with site 4.	47
B9. Spatial coherency as function of distance at some representative frequencies for signals (solid) and noise (dashed) at MINA, GABBS, LLNL, and GAR sites. .	48

LIST OF TABLES

TABLE #	PAGE
1 Site Locations of the Noise Survey.	5
2 General Information.	8
3. PSD (Day/Night) Comparisons at 1 Hz and 6 Hz.	14

ACKNOWLEDGMENTS

Data for MINA and GABBS were provided by the AlliedSignal Technical Services Corp. Data for GAR were provided by the Southern Methodist University (SMU). Data for the Excelsior Mountains (near MINA) and at sites east of GAR were provided by Lawrence Livermore National Laboratory (LLNL). Dr. Robert Kemerait, Mr. Thomas Kelly, Mr. John Dwyer, and Mr. Jon Creasey of CTI assisted with the information on the data and coordination with the above groups to effectively make the data delivery as fast and as smooth as possible. Ms. Stephanie Fisher provided editorial and administrative reviews.

ABSTRACT

Noise was analyzed for displacement power spectral density (PSD) in decibels (dB) referred to units of nanometers (nm)²/Hertz (Hz) from noise time series acquired in 1997, days 216-224, in the state of Nevada, USA, at MINA seismic stations, GABBS Valleys, Excelsior Mountains, GAR seismic stations, and nearby to the east of GAR seismic stations. The noise survey at MINA seismic stations and GABBS Valleys were conducted by the AlliedSignal Technical Services Corp. with four sites at each location. The noise survey to the east of GAR seismic stations composed of four sites and at the Excelsior Mountains near MINA composed of two sites were conducted by the Lawrence Livermore National Laboratory (LLNL). The Southern Methodist University (SMU) conducted the noise surveys at the existing locations of GAR seismic stations. AlliedSignal employed the Teledyne Geotech GS-13 seismometer and the RDAS-200P digitizer for their noise survey. LLNL and SMU used the GS-13 and the REFTEK digitizer. The PSD results at 1 Hz and 6 Hz are as follows:

Name	Latitude (°)	Longitude (°)	Displacement Power Spectral Density in dB referred to 1 nm ² /Hz (Day/Night)	Standard Deviation (Day/Night)	Noise RMS Amplitude (nm) (0.8-3.0 Hz)	Noise Surveyed By
			1 Hz	1 Hz		
			6 Hz	6 Hz		
MINA, Site 1	38.2758	-118.4710	-2.5/-9.0 -26.7/-32.7	5.4/5.8 6.3/7.6	0.62/0.33	AlliedSignal
MINA, Site 2	38.2796	-118.4740	-5.5/-9.2 -34.7/-40.1	4.3/4.3 11.1/7.5	0.45/0.31	AlliedSignal
MINA, Site 3	38.2736	-118.4660	-0.2/-6.8 -25.6/-32.0	6.2/6.2 8.2/9.7	0.82/0.41	AlliedSignal
MINA, Site 4	38.2735	-118.4750	-4.2/-9.5 -40.5/-45.3	5.3/5.3 6.5/6.5	0.53/0.27	AlliedSignal
GABBS, Site 1	38.6191	-118.2260	-7.2/-0.5 -40.1/-31.2	8.0/8.0 5.0/9.9	0.37/0.78	AlliedSignal
GABBS, Site 2	38.6192	-118.2300	-1.4/-8.5 -34.9/-38.5	4.7/4.7 5.2/5.7	0.72/0.33	AlliedSignal

Name	Latitude (°)	Longitude (°)	Displacement Power Spectral Density in dB referred to 1 nm ² /Hz (Day/Night)	Standard Deviation (Day/Night)	Noise RMS Amplitude (nm) (0.8-3.0 Hz)	Noise Surveyed By
			1 Hz	1 Hz		
			6 Hz	6 Hz		
GABBS, Site 3	38.6240	-118.2280	1.9/1.2 -34.9/-33.4	8.9/8.9 6.2/11.5	1.07/0.94	AlliedSignal
GABBS, Site 4	38.6179	-118.2200	-0.8/-5.9 -36.1/-35.8	6.8/4.3 5.3/6.4	0.77/0.42	AlliedSignal
LLNL, Site 1	38.4387	-118.2139	4.2/-8.2 -31.0/-36.5	8.6/12.4 9.7/14.1	0.51/0.32	LLNL
LLNL, Site 3	38.4208	-118.1900	-9.3/-12.9 -32.0/-37.4	9.9/14.5 9.6/14.8	0.33/0.21	LLNL
LLNL, Site 4	38.4150	-118.2106	-4.5/-5.0 -28.9/-30.7	4.7/4.0 6.4/4.8	0.51/0.48	LLNL
LLNL, Site 6	38.4336	-118.2193	-5.2/-5.7 -30.2/-32.3	4.6/4.2 6.2/5.3	0.54/0.52	LLNL
Excelsior Mountains, Site1	38.279	-118.4734	-2.3/-6.0 -33.9/-39.2	7.1/7.1 7.8/9.8	0.65/0.43	LLNL
Excelsior Mountains, Site2	38.2737	-118.4749	-7.4/-8.8 -39.1/-44.3	4.7/3.2 5.8/5.7	0.36/0.31	LLNL
GARA0	38.4268	-118.3000	-8.8/-8.9 -31.0/-33.0	3.7/4.4 4.3/4.6	0.33/0.33	SMU
GARB1	38.4240	-118.3063	-9.6/-9.8 -30.2/-32.5	3.1/3.6 5.3/5.0	0.33/0.32	SMU
GARB2A	38.4208	-118.2898	-9.7/-11.1 -33.7/-37.6	2.3/1.8 7.1/2.0	0.28/0.25	SMU
GARB2	38.4258	-118.2908	-10.8/-11.2 -37.3/-39.3	3.3/3.6 3.8/3.9	0.26/0.25	SMU
GARB3	38.4342	-118.3043	-12.6/-12.3 -40.8/-42.3	2.5/3.0 3.8/3.9	0.21/0.21	SMU
GARBL1	38.4502	-118.2933	-13.5/-13.6 -44.1/-46.5	2.2/2.0 3.5/3.7	0.18/0.18	SMU
GARC4	38.4105	-118.2952	-8.8/-10.0 -35.1/-37.6	4.4/4.9 4.9/5.3	0.30/0.27	SMU

These results can be compared with the United States Geological Survey's (USGS's) New Low and High Noise Models (NLNM and NHNM) which give -18 and 32 dB re nm²/Hz at 1 Hz, respectively.

With respect to mean PSD values at 1 Hz, GABBS Valleys Site 3 is noisiest with daytime and nighttime noise at +1.9 and +1.2 dB, respectively. Furthermore, the noise levels at sites that are much quieter are LLNL Site 3 east of GAR seismic stations with daytime and nighttime noise levels at -9.3 and -12.9 dB, respectively; and GARB3 with daytime and nighttime noise levels at -12.6 and -12.3 dB, respectively. The site at GARBL1 is the quietest site in this survey with daytime and nighttime noise levels at -13.5 and -13.6 dB, respectively.

With respect to mean PSD values at 6 Hz, daytime noise at MINA Site 3 is noisiest with a value of -25.6 dB. Furthermore, the noise levels at sites that are much quieter at night are MINA Site 4 and LLNL Excelsior Mountains Site 2 with nighttime noise levels at -45.3 and -44.3 dB, respectively. The site at GARBL1 is the quietest site in this survey with daytime and nighttime noise levels at -44.1 and -46.5 dB, respectively.

Signal Coherence Spectra: Signal coherence is excellent with most of coherence values near unity at MINA up to about 2 Hz. Beyond 2 Hz, signal coherency is not interpretable. Good signal coherency is found for other sites such as GABBS, GAR, and LLNL sites. Signal coherency is representable and interpretable at these sites.

Noise Coherence Spectra: Noise coherency is good at GAR and LLNL sites; poorer noise coherency is at MINA and GABBS. Noise coherency is representable and interpretable at these sites.

INTRODUCTION

This report is written to record the results of noise spectra obtained from the seismic noise time series acquired in 1997, days 216-224, in the state of Nevada, USA, at MINA seismic stations, GABBS Valleys, Excelsior Mountains, GAR seismic stations, and nearby to the east of GAR seismic stations. The noise surveys at MINA seismic stations and GABBS Valleys were conducted by the AlliedSignal Aerospace/AlliedSignal Technical Services Corp. with four sites at each location. The noise survey to the east of GAR seismic stations composed of four sites and at the Excelsior Mountains (near MINA) composed of two sites were conducted by the Lawrence Livermore National Laboratory (LLNL). The Southern Methodist University (SMU) conducted the noise surveys at the proximity of the existing locations of GAR seismic stations. Figure 1 shows the map indicating the locations of these noise-survey sites. Table 1 lists the locations of these sites.

MAP OF NOISE SURVEY DAYS 216-224 YEAR 1997-WHOLE PART

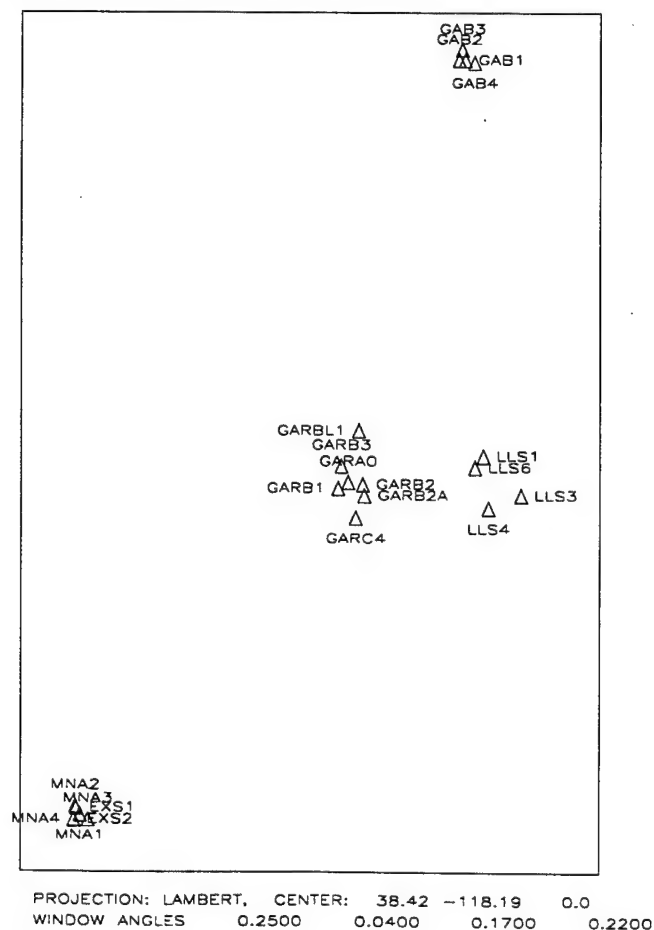


Figure 1. Site locations of noise survey in Nevada, USA, days 216-224, year 1997.

Table 1: Site Locations of the Noise Survey

SITES	Latitude (°)	Longitude (°)	Surveyed By
MNA1	38.2758	-118.4710	AlliedSignal
MNA2	38.2796	-118.4740	AlliedSignal
MNA3	38.2736	-118.4660	AlliedSignal
MNA4	38.2735	-118.4750	AlliedSignal
GAB1	38.6191	-118.2260	AlliedSignal
GAB2	38.6192	-118.2300	AlliedSignal
GAB3	38.6240	-118.2280	AlliedSignal
GAB4	38.6179	-118.2200	AlliedSignal
LLS1	38.4387	-118.2139	LLNL
LLS3	38.4208	-118.1900	LLNL
LLS4	38.4150	-118.2106	LLNL
LLS6	38.4336	-118.2193	LLNL
EXS1	38.27896	-118.47339	LLNL
EXS2	38.27374	-118.47490	LLNL
GARA0	38.4268	-118.3000	SMU
GARB3	38.4342	-118.3043	SMU
GARB1	38.4240	-118.3063	SMU
GARBL1	38.4502	-118.2933	SMU
GARB2A	38.4208	-118.2898	SMU
GARC4	38.4105	-118.2952	SMU
GARB2	38.4258	-118.2908	SMU

The AlliedSignal Aerospace/AlliedSignal Technical Services Corp. employed the Tele-dyne Geotech GS-13 seismometer and the RDAS-200P digitizer for their noise survey. LLNL and SMU used the GS-13 and the REFTEK digitizer.

PURPOSE

The purpose is to investigate the characteristics of noise for site selection in order to set up an International Monitoring System (IMS) station for use under the Comprehensive Test Ban Treaty (CTBT).

INSTRUMENT RESPONSES

The instrument response of the GS-13/RDAS-200P employed for this noise survey follows that of the Designated Seismic Station (DSS) Vault Seismic System (VSS)¹ [pages 1-6]. The velocity sensitivity is 22.44 counts/nanometers(nm)/second (sec) at 1 Hz for the GS-13/RDAS-200P system for sites surveyed by AlliedSignal. For the GS-13/REFTEK system, the high-gain displacement sensitivity² employed at GAR seismic station sites is known as 0.004897 nm/count (or 204.21 counts/nm) at 1 Hz for sites surveyed by SMU; the displacement sensitivity³ is 844 counts/nm at 4 Hz for sites surveyed by LLNL. In particular, for the instrument response of GS-13/REFTEK system, the assumption has been that the REFTEK digitizer's response is flat at the frequencies of interest. The normalized velocity and displacement amplitude system responses for the GS13/RDAS-200P and GS13/REFTEK, respectively, are shown in Figure 2.

Noise seismograms were corrected for instrument response with the *displacement* system response of the GS13/REFTEK for data provided by the SMU and LLNL groups. The noise ground motion seismograms then become *displacement* noise ground motion seismograms. Noise seismograms which were corrected for the *velocity* system response of the GS13/RDAS-200P for data provided by the AlliedSignal group become *velocity* noise ground motion seismograms. The discussion on what becomes of a ground motion seismogram after an instrument system response correction has been both theoretically treated and exemplified⁴.

1. Teledyne Geotech, *Designated Seismic Station (DSS) Vault Seismic System (VSS) - User's Guide*, Document Number 990-59300-9800, Teledyne Geotech, P.O. Box 469007, Garland TX 75046-9007, 1 July 1992.

2. Personal communication via e-mail between Paul Golden of SMU and Tom Kelly of CTI dated 3 September 1997.

3. Personal communication via e-mail between LLNL and Tom Kelly of CTI dated 3 September 1997.

4. Bao V. Nguyen (1995). The instrument responses of the SKM-3 System and the Designated Seismic Station Vault Seismic System, *Bull. Seism. Soc. Am.* 85, 1835-1846.

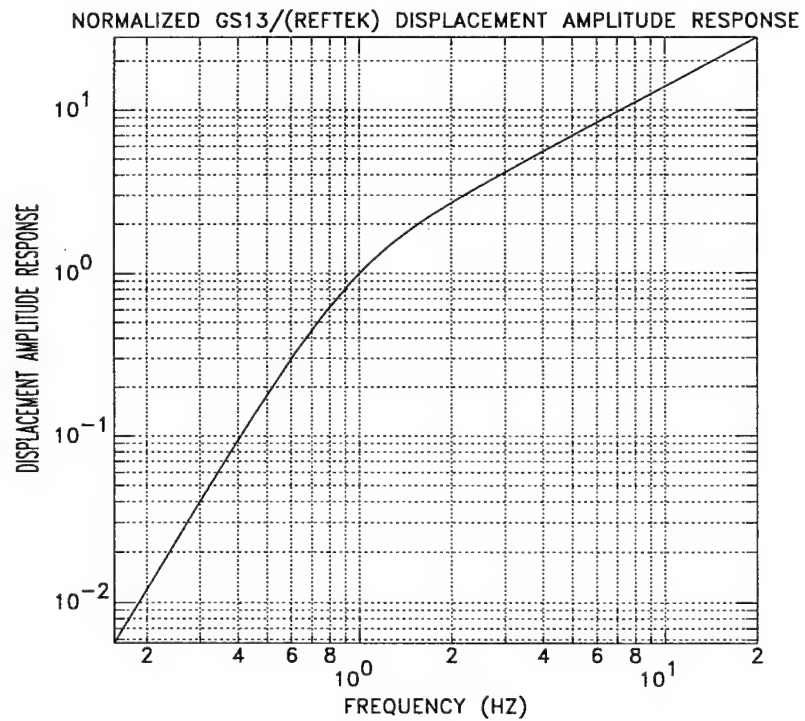
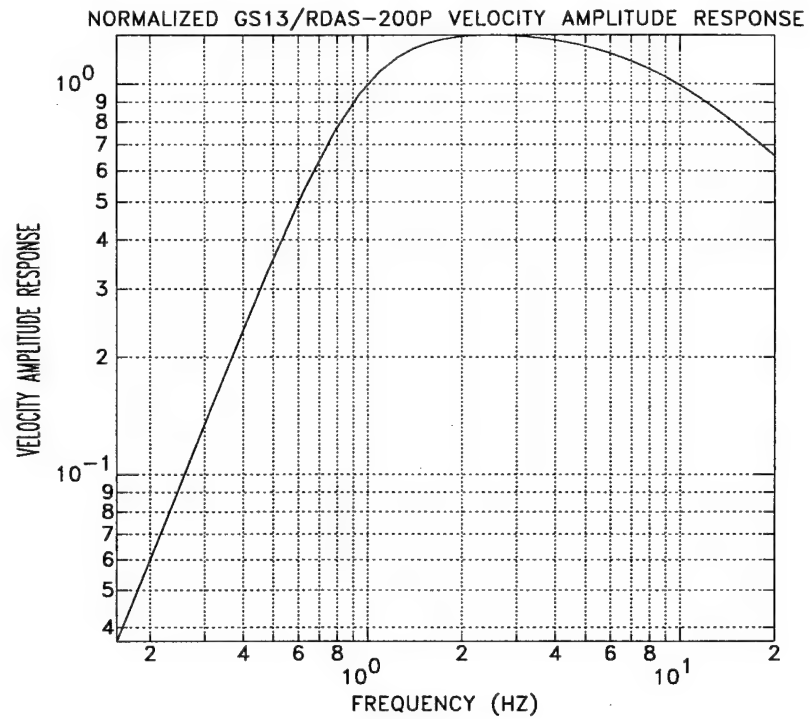


Figure 2. The normalized velocity and displacement amplitude system responses for the GS13/RDAS-200P and GS13/REFTEK, respectively.

NOISE ANALYSIS

The individual instrument-corrected noise time series were analyzed employing averaging time domain correlations over a set of data segments after windowing. Subsequently, the average auto-correlation function was Fourier transformed to obtain *power spectral density*. Specifically, an auto-correlation function was computed for each segment of 10 seconds in length and segments were overlapped by 50%. For each segment, the windowing was performed with a *Hanning* windowing function. The collection of windowed auto-correlation functions was then averaged over a set of data segments (windows) and fast Fourier transformed to obtain power spectral density (PSD). In practice, double instrument corrections were performed on the noise power amplitudes after obtaining the auto-correlation function to avoid numerical instability resulting from edge effects of instrument response correction.

From the paragraph above, the *average* and *standard deviation* of power spectral density were computed based on employed noise time series analyzed for each site.

Table 2 lists general information.

Table 2: General Information

Name	Date of Recordings (Year 1997)	Sampling Rate (samples/sec)	Length of Noise Time Series used in PSD (sec)	Measurements made at	Noise Surveyed By
MINA, Site 1	220-223	40	300		AlliedSignal
MINA, Site 2	220-224	40	300		AlliedSignal
MINA, Site 3	220-224	40	300		AlliedSignal
MINA, Site 4	220-224	40	300		AlliedSignal
GABBS, Site 1	228-230	40	300	Open ground, weathered granite	AlliedSignal
GABBS, Site 2	228-230	40	300	Open ground, weathered granite	AlliedSignal

Table 2: General Information (Continued)

Name	Date of Recordings (Year 1997)	Sampling Rate (samples/sec)	Length of Noise Time Series used in PSD (sec)	Measurements made at	Noise Surveyed By
GABBS, Site 3	228-230	40	300	Open ground, weathered granite	AlliedSignal
GABBS, Site 4	228-230	40	300	Open ground, weathered granite	AlliedSignal
LLNL, Site 1	219-223	40	300		LLNL
LLNL, Site 3	219-223	40	300		LLNL
LLNL, Site 4	219-223	40	300		LLNL
LLNL, Site 6	219-223	40	300		LLNL
LLNL, Excelsior Site 1	219-223	40	300		LLNL
LLNL, Excelsior Site 2	219-223	40	300		LLNL
GARA0	216-223	40	300	Lithified conglomerate	SMU
GARB1	216-223	40	300	Lithified conglomerate	SMU
GARB2A	217-218	40	300		SMU
GARB2	218-223	40	300	Alluvium	SMU
GARB3	216-224	40	300	Limestone	SMU
GARBL1	217-223	40	300	Limestone	SMU
GARC4	217-223	40	300	Sandstone	SMU

COMPARISONS

Since 1993, the United States Geological Survey (USGS) has had a set of new noise models: NLNM (New Low Noise Model) and NHNM (New High Noise Model).¹ These noise models were obtained by graphically fitting straight line segments to the lower and upper envelopes of the spectral overlay of many networks of stations such as the SRO (Seismic Research Observatories) systems, the ASRO systems which are updated versions of the High Gain Long Period (HGLP) seismographs, the Digital World-Wide Standardized Seismograph Network (DWWSSN), the Chinese Digital Seismograph Network (CDSN), the IRIS/USGS (Incorporated Research Institutions for Seismology) systems, the IRIS/IDA (International Deployment of Accelerometers) systems, the Regional Seismic Test Network (RSTN) systems, and TERRAscope systems. In the words of Peterson, "the NLNM is a composite of station spectra obtained from many different instruments, vaults, geologic environments, and geographic regions," and represents "a hypothetical background spectrum that is unlikely to be duplicated at any single location on Earth. The NHNM is a spectrum of average high background noise power in the network. Clearly, one can find sites that are noisier or periods of time at stations in the network that may be affected by microseismic storms or by increased local activities that disturb the instruments." The models plotted in Figures A1-A42 of Appendix A serve as benchmarks against which other noise power spectral densities can be compared. At 1 Hz, the NLNM is at -18 dB (referred to displacement power spectral density in $1 \text{ nm}^2/\text{Hz}$); the NHNM is at about 32 dB.

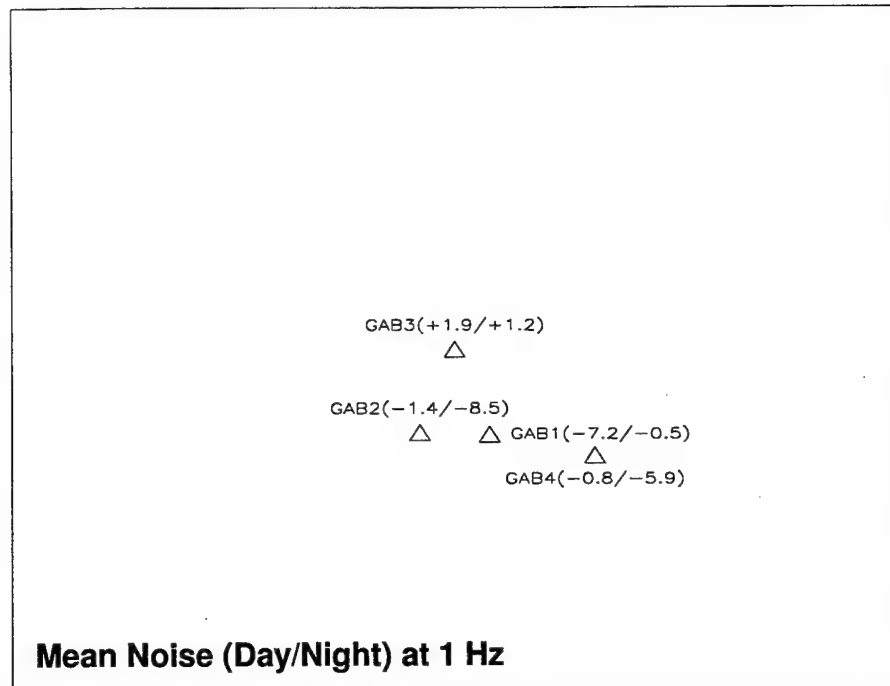
Table 3 lists PSD (Day/Night) comparisons at 1 Hz and 6 Hz for all sites analyzed in this report.

Figures 3a-c show the upper part, middle part, and lower part of the noise survey map as seen from Figure 1 indicating the displacement power spectral density (daytime and nighttime, respectively) at 1 Hz and 6 Hz at these sites.

Figures A1-A42 of Appendix A show noise power spectral densities obtained from these sites.

1. Jon Peterson (1993). *Observations and Modeling of Seismic Background Noise*, Open-File Report 93-322, Albuquerque, New Mexico, U.S. Department of Interior Geological Survey.

MAP OF NOISE SURVEY DAYS 216-224 YEAR 1997-UPPER PART



MAP OF NOISE SURVEY DAYS 216-224 YEAR 1997-UPPER PART

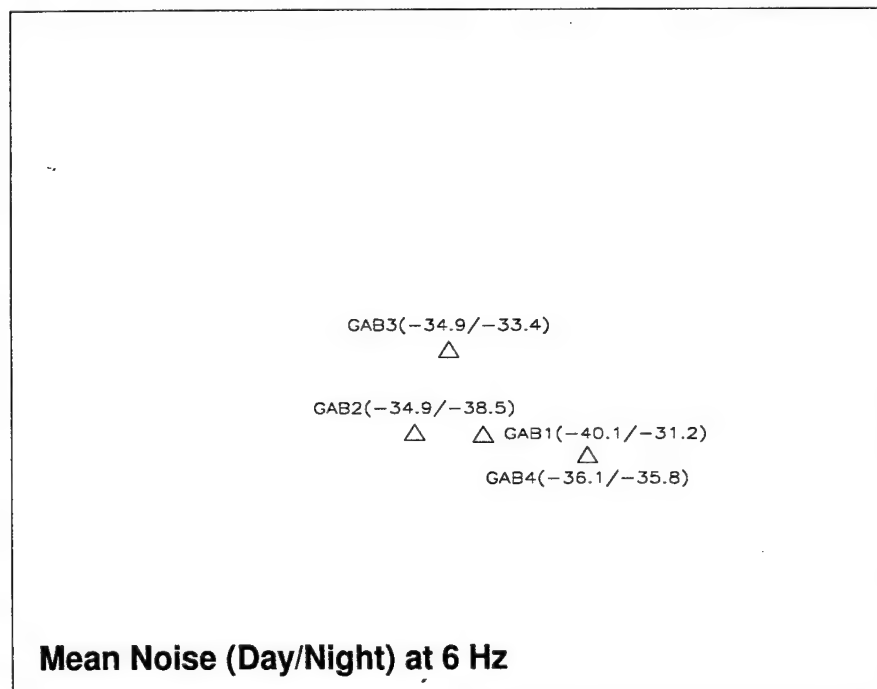
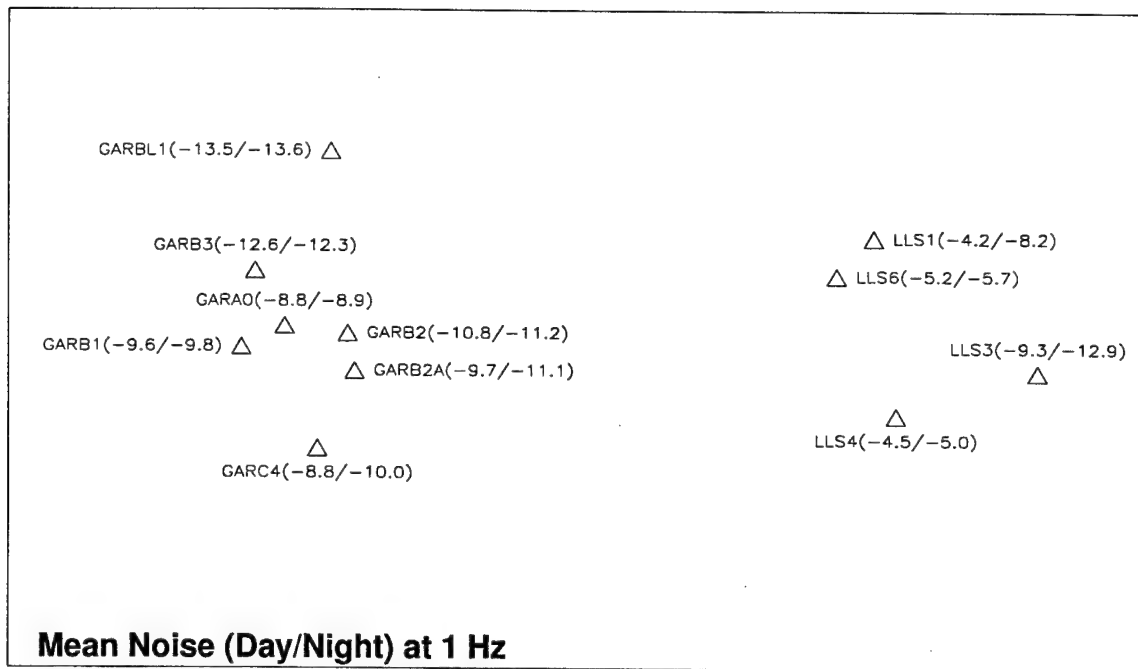


Figure 3a. Map of noise survey days 216-224 year 1997-upper part-showing PSD values (Day/Night) in dB (re nm^2/Hz) at 1 Hz and 6 Hz, respectively.

MAP OF NOISE SURVEY DAYS 216-224 YEAR 1997-MIDDLE PART



MAP OF NOISE SURVEY DAYS 216-224 YEAR 1997-MIDDLE PART

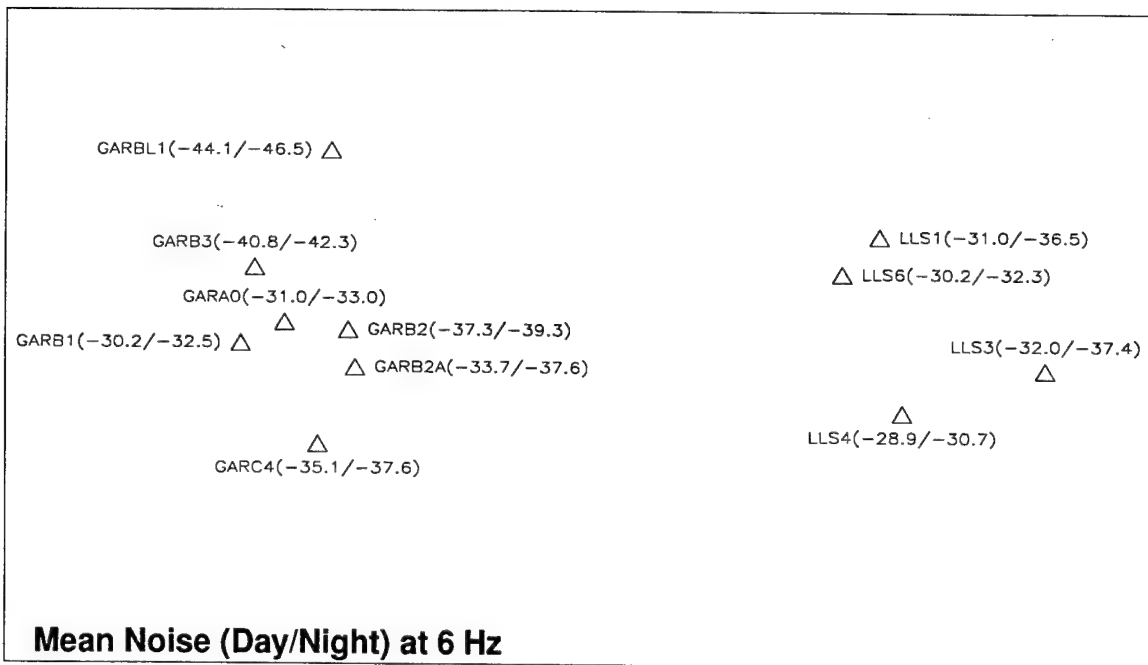
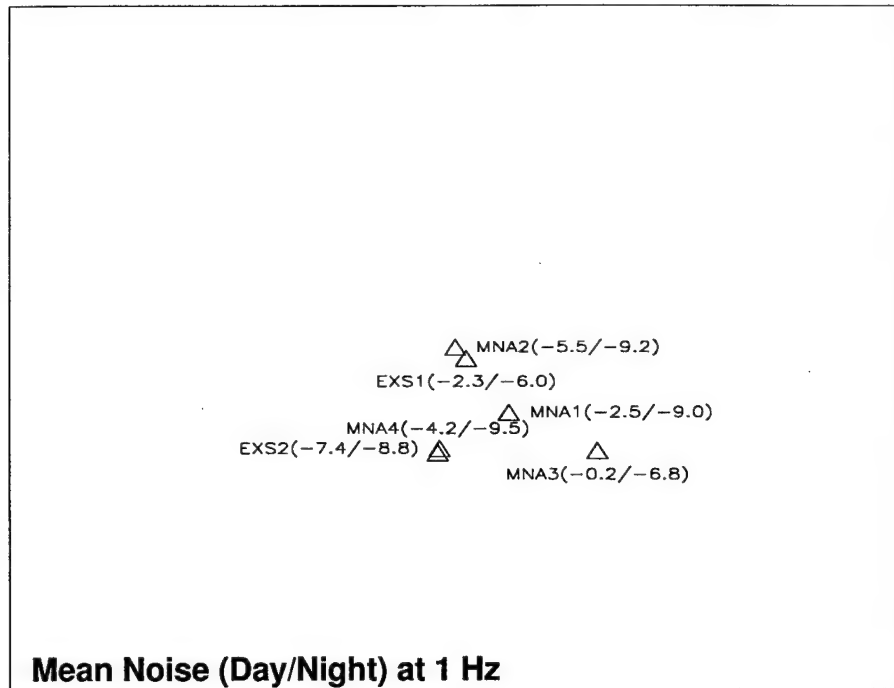


Figure 3b. Map of noise survey days 216-224 year 1997-middle part-showing PSD values (Day/Night) in dB (re nm²/Hz) at 1 Hz and 6 Hz, respectively.

MAP OF NOISE SURVEY DAYS 216-224 YEAR 1997-LOWER PART



MAP OF NOISE SURVEY DAYS 216-224 YEAR 1997-LOWER PART

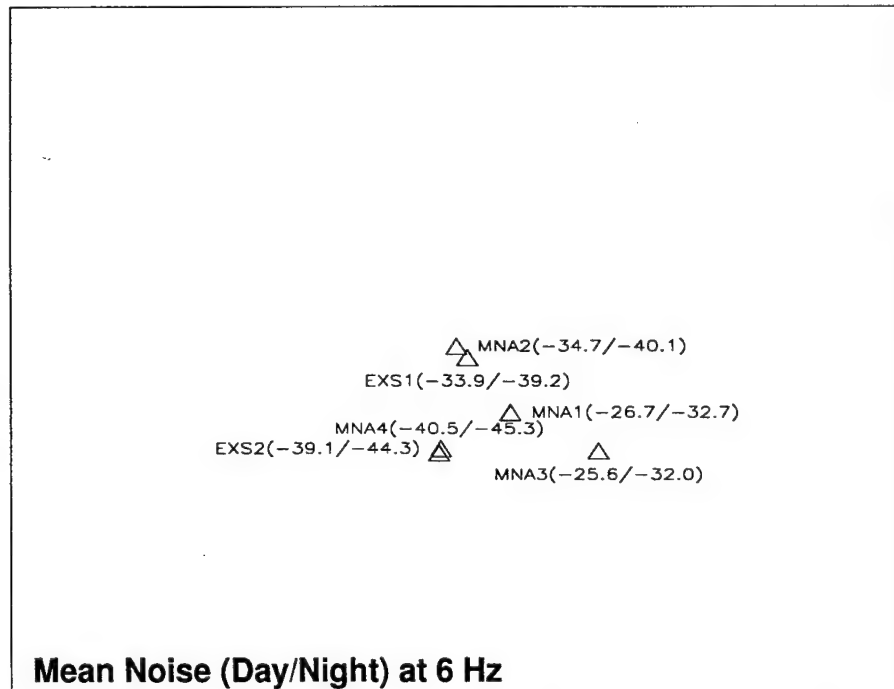


Figure 3c. Map of noise survey days 216-224 year 1997-lower part-showing PSD values (Day/Night) in dB (re nm²/Hz) at 1 Hz and 6 Hz, respectively.

Table 3: PSD (Day/Night) Comparisons at 1 Hz and 6 Hz

Name	Displ. PSD in dB re nm ² /Hz	Standard Deviation	Normalized Noise PSD	Displ. PSD in dB re nm ² /Hz	Standard Deviation	Normalized Noise PSD	Noise RMS Amplitude (nm)
	(1 Hz)			(6 Hz)			(0.8-3.0 Hz)
NLNM	-18	-	0.22	-	-	-	-
NHNM	32	-	22380.0	-	-	-	-
Lajitas, Texas ^a	(-11.5) [-9]	- -	1.00 1.78	- [-45.16]	- -	- 1.00	- -
Pinedale ^b	-18.2 [-2.8]	5.7 [12.4]	0.21 7.40	- -	- -	- -	0.16 -
Dubna ^c	-21.5	2.3	0.10	-	-	-	0.19
MINA, Site 1	-2.5/-9.0	5.4/5.8	7.94/1.78	-26.7/-32.7	6.3/7.6	70.15/17.62	0.62/0.33
MINA, Site 2	-5.5/-9.2	4.3/4.3	3.98/1.70	-34.7/-40.1	11.1/7.5	11.12/3.21	0.45/0.31
MINA, Site 3	-0.2/-6.8	6.2/6.2	13.49/2.95	-25.6/-32.0	8.2/9.7	90.36/20.70	0.82/0.41
MINA, Site 4	-4.2/-9.5	5.3/5.3	5.37/1.58	-40.5/-45.3	6.5/6.5	2.92/0.97	0.53/0.27
GABBS, Site 1	-7.2/-0.5	8.0/8.0	2.69/12.59	-40.1/-31.2	5.0/9.9	3.21/24.89	0.37/0.78
GABBS, Site 2	-1.4/-8.5	4.7/4.7	10.23/2.00	-34.9/-38.5	5.2/5.7	10.62/4.63	0.72/0.33
GABBS, Site 3	1.9/1.2	8.9/8.9	21.88/18.62	-34.9/-33.4	6.2/11.5	10.62/15.00	1.07/0.94
GABBS, Site 4	-0.8/-5.9	6.8/4.3	11.75/3.63	-36.1/-35.8	5.3/6.4	8.05/8.63	0.77/0.42
LLNL, Site 1	-4.2/-8.2	8.6/12.4	5.37/2.14	-31.0/-36.5	9.7/14.1	26.06/7.35	0.51/0.32
LLNL, Site 3	-9.3/-12.9	9.9/14.5	1.66/0.72	-32.0/-37.4	9.6/14.8	20.70/5.97	0.33/0.21
LLNL, Site 4	-4.5/-5.0	4.7/4.0	5.01/4.47	-28.9/-30.7	6.4/4.8	42.27/27.93	0.51/0.48
LLNL, Site 6	-5.2/-5.7	4.6/4.2	4.27/3.80	-30.2/-32.3	6.2/5.3	31.33/19.32	0.54/0.52
LLNL, Excel- sior Site1	-2.3/-6.0	7.1/7.1	8.32/3.55	-33.9/-39.2	7.8/9.8	13.37/3.94	0.65/0.43
LLNL, Excel- sior Site2	-7.4/-8.8	4.7/3.2	2.57/1.86	-39.1/-44.3	5.8/5.7	4.04/1.22	0.36/0.31
GARA0	-8.8/-8.9	3.7/4.4	1.86/1.82	-31.0/-33.0	4.3/4.6	26.06/16.44	0.33/0.33
GARB1	-9.6/-9.8	3.1/3.6	1.55/1.48	-30.2/-32.5	5.3/5.0	31.33/18.45	0.33/0.32

Table 3: PSD (Day/Night) Comparisons at 1 Hz and 6 Hz (Continued)

Name	Displ. PSD in dB re nm ² /Hz	Standard Deviation	Normalized Noise PSD	Displ. PSD in dB re nm ² /Hz	Standard Deviation	Normalized Noise PSD	Noise RMS Amplitude (nm)
	(1 Hz)			(6 Hz)			(0.8-3.0 Hz)
GARB2A	-9.7/-11.1	2.3/1.8	1.51/1.10	-33.7/-37.6	7.1/2.0	14.00/5.70	0.28/0.25
GARB2	-10.8/-11.2	3.3/3.6	1.17/1.07	-37.3/-39.3	3.8/3.9	6.11/3.85	0.26/0.25
GARB3	-12.6/-12.3	2.5/3.0	0.78/0.83	-40.8/-42.3	3.8/3.9	2.73/1.93	0.21/0.21
GARBL1	-13.5/-13.6	2.2/2.0	0.63/0.62	-44.1/-46.5	3.5/3.7	1.28/0.73	0.18/0.18
GARC4	-8.8/-10.0	4.4/4.9	1.86/1.41	-35.1/-37.6	4.9/5.3	10.14/5.70	0.30/0.27

- a. Values in parentheses are in dB referred to 1 nm²/Hz. Values in brackets are given by Ms. Carol Finn (personal communication) for PSD in dB referred to 1 nm²/Hz at 1 Hz for the Pinedale Array noise spectra recorded by the short period instruments model 23900. In addition, for Lajitas, TX, noise spectra were recorded by the TXAR.
- b. Bao V. Nguyen (1996). Noise power spectral density estimates at Ukrainian site (Makarov), USA site (Pinedale, Wyoming), and Russian sites (Dubna, Peleduy, Ussuriysk, Zalesovo, and near Bilibino), AFTAC, TTR-TN-96-001, 52 pp.
- c. Ibid.

COHERENCE ESTIMATES

*Coherence function*¹ is a real-valued quantity defined as the ratio of the squared magnitude of the one-sided cross spectrum of the two time series to the product of their one-sided auto spectra and is varied between 0 and 1, inclusive. The coherence function is analogous to the squared correlation coefficient function but is not equal to its Fourier transform. The *correlation coefficient function*² is defined as the ratio of the cross-covariance function of lag time between the two time series to the square root of their product of the auto-covariance functions at zero lag time. The absolute value of the correlation coefficient is less than or equal to 1, inclusive. Mean values different from zero should be removed from the data before computing coherence function to eliminate delta function behavior at the origin³.

1. Julius S. Bendat and Allan G. Piersol (1980). *Engineering Applications of Correlation and Spectral Analysis*, John Wiley & Sons, 302 pp.

2. Ibid.

3. Ibid.

In computing correlation coefficients, the two time series are to be narrow-band passed at each center frequency and the auto- and cross-correlation functions are to be windowed with a window applied to the entire time series length. Normalization is then performed with respect to the maximum amplitude of the auto-correlation function. On the other hand, in computing coherence function in this report, the auto- and cross-correlation functions were windowed with a triangular window applied to each segment, and the segments were overlapped by 65% prior to averaging and Fourier transforming.

Noise is assumed stationary and random; whereas, signal is transient, short in duration, and is assumed to be nonstationary phenomenon with a clearly defined beginning and end. In this report, coherence function is employed for noise coherence estimates from 15-second pre-signal noise time series of each elemental site; whereas, coherence function is employed for signal coherence estimates from 4-second time series for P waves of each elemental site assuming a stochastic process being at work.

Figures B1, B3, B5, B7, and B9 of Appendix B show signal and pre-signal noise coherence as functions of frequency (coherence) and distance (spatial coherence) relative to some reference site. Figures B2, B4, B6, and B8 show spectral multiplications for signals as well as for pre-signal noise of the corresponding elemental sites with some corresponding reference site. These spectral-multiplications figures aid in interpreting the aforementioned coherence estimates of noise and signals of Figures B1, B3, B5, and B7. For example, in Figures B1 and B2 for MINA, excellent signal coherence with values near unity is seen up to about 2 Hz. The signal coherence values drop for frequencies greater than about 2 Hz. But greater than about 2 Hz, the levels of the signal spectral products are about those of the noise spectral products. What can be said of signal coherence estimates for frequencies greater than about 2 Hz at MINA sites is that they are not interpretable. On the other hand, the noise coherence estimates are representable since the noise spectral products exist up to and dropped off at the Nyquist frequency. Similar interpretations can be used to apply to Figures B3 and B4 for GABBS, B5 and B6 for GAR, and B7 and B8 for LLNL sites. Both the signal and noise coherence estimates for GABBS, GAR, and LLNL sites are representable and interpretable up to the Nyquist frequency.

Figure B9 shows spatial coherence varying with distance of elemental sites relative to some reference site evaluated at some representative frequencies. Since only few elemental sites were available, spatial coherency for MINA, GABBS, GAR, and LLNL sites is not meaningful enough for further interpretation and comparison.

DISCUSSIONS AND CONCLUSIONS

Noise Analysis

The overall results of analysis indicate noise power spectral densities at these sites are low with PSD values ranging from +1.9 to -13.6 dB re nm^2/Hz at 1 Hz and from -25.6 to -46.5 dB at 6 Hz.

Low amplification of noise is seen at 3.5 Hz, 9 Hz, and 16 Hz at MINA Site 2; 2.0 Hz, 3.5 Hz, and 8.5 Hz at MINA Site 4.

Low amplification of noise is seen for GABBS Valley Sites 1 and 3 at 16 Hz; 8 Hz at Site 3 for mostly nighttime; 8 Hz and 15 Hz at Site 2 for nighttime; 3.5 Hz and 4.0 Hz at Site 4.

Low amplification of noise is seen for LLNL Site 6 at 16 Hz; 3.5 Hz and 4.0 Hz at Sites 1, 3, and 6; 3.5 Hz at Site 4; 8 Hz at Site 1; 9 Hz at Site 6.

Low amplification of noise is seen for LLNL Excelsior Mountains Sites 1 and 2 (near MINA) at 3.5 Hz; 8 Hz at Site 2; 9.5 Hz at Site 1; 12 Hz at Site 2.

Low amplification of noise is seen for SMU GAR Sites A0, B1, B2, B2A, B3, BL1, and C4 at 3.5 Hz; 4.0 Hz at A0, B2, BL1, and C4; 8 Hz at A0, B1, B2, B2A, BL1, and C4; 12 Hz at A0, B1 and B2.

With respect to mean PSD values at 1 Hz, GABBS Valleys Site 3 is noisiest with daytime and nighttime noise at +1.9 and +1.2 dB, respectively. Furthermore, the noise levels at

sites that are much quieter are LLNL Site 3 east of GAR seismic stations with daytime and nighttime noise levels at -9.3 and -12.9 dB, respectively; GARB3 with daytime and nighttime noise levels at -12.6 and -12.3 dB, respectively. The site at GARBL1 is the quietest site in this survey with daytime and nighttime noise levels at -13.5 and -13.6 dB, respectively.

With respect to mean PSD values at 6 Hz, daytime noise at MINA Site 3 is noisiest with a value of -25.6 dB. Furthermore, the noise levels at sites that are much quieter at night are MINA Site 4 and LLNL Excelsior Mountains Site 2 with nighttime noise levels at -45.3 and -44.3 dB, respectively. The site at GARBL1 is the quietest site in this survey with daytime and nighttime noise levels at -44.1 and -46.5 dB, respectively.

Figure 4 shows a composite of noise levels at 1 Hz and 6 Hz for all the sites of this noise survey.

Coherence Analysis

Signal Coherence Spectra: Signal coherence is excellent with most of coherence values near unity at MINA up to about 2 Hz. Beyond 2 Hz, signal coherency is not interpretable. Good signal coherency is found for other sites such as GABBS, GAR, and LLNL sites. Signal coherency is representable and interpretable at these sites.

Noise Coherence Spectra: Noise coherency is good at GAR and LLNL sites; poorer noise coherency is at MINA and GABBS. Noise coherency is representable and interpretable at these sites.

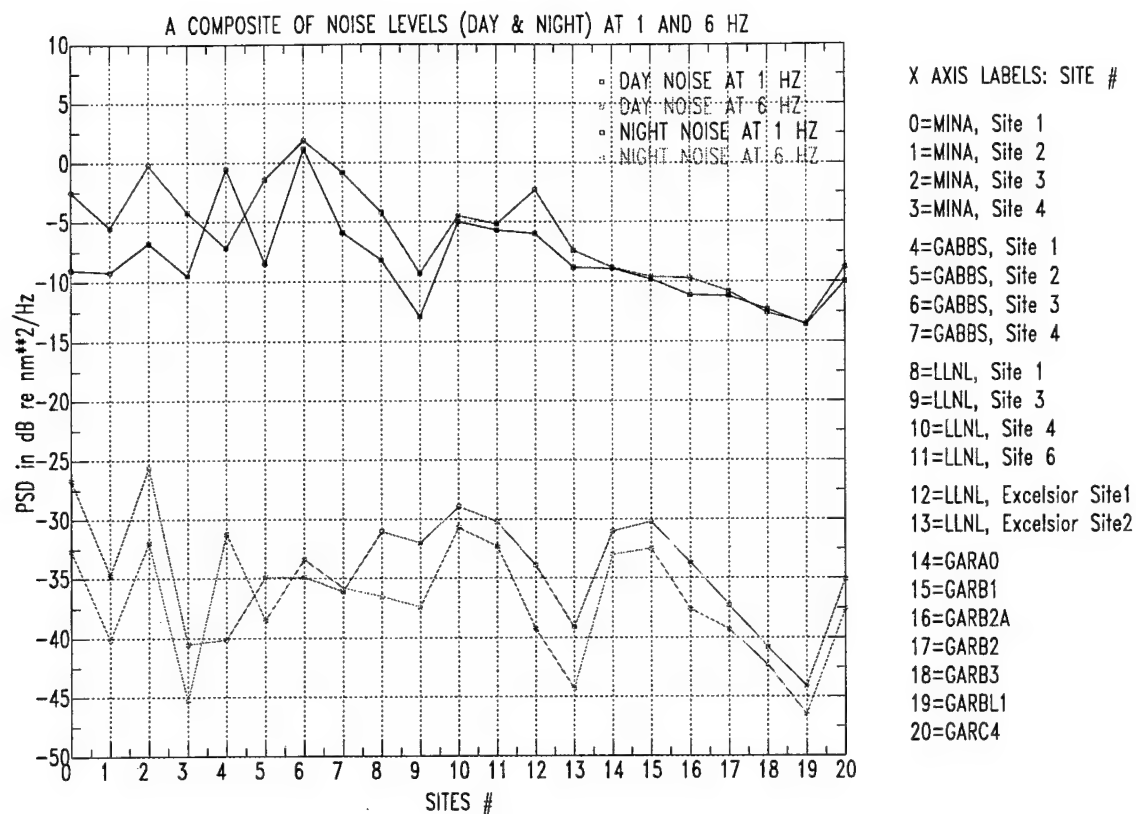


Figure 4. A composite of mean noise levels (day and night) at 1 Hz and 6 Hz for all the sites of this noise survey.

REFERENCES

- Bendat, Julius S., and Allan G. Piersol (1980). Engineering Applications of Correlation and Spectral Analysis, John Wiley & Sons, 302 pp.
- Nguyen, Bao V. (1995). The instrument responses of the SKM-3 System and the Designated Seismic Station Vault Seismic System, *Bull. Seism. Soc. Am.* **85**, 1835-1846.
- Nguyen, Bao V. (1996). *Noise power spectral density estimates at Ukrainian site (Makarov), USA site (Pinedale, Wyoming), and Russian sites (Dubna, Peleduy, Ussuriysk, Zalesovo, and near Bilibino)*, AFTAC, **TTR-TN-96-001**, 52 pp.
- Peterson, Jon (1993). *Observations and Modeling of Seismic Background Noise*, **Open-File Report 93-322**, Albuquerque, New Mexico, US Department of Interior Geological Survey.
- Teledyne Geotech, *Designated Seismic Station (DSS) Vault Seismic System (VSS) - User's Guide*, **Document Number 990-59300-9800**, Teledyne Geotech, P.O. Box 469007, Garland TX 75046-9007, 1 July 1992.

APPENDIX A:
PLOTS OF DISPLACEMENT POWER SPECTRAL DENSITY

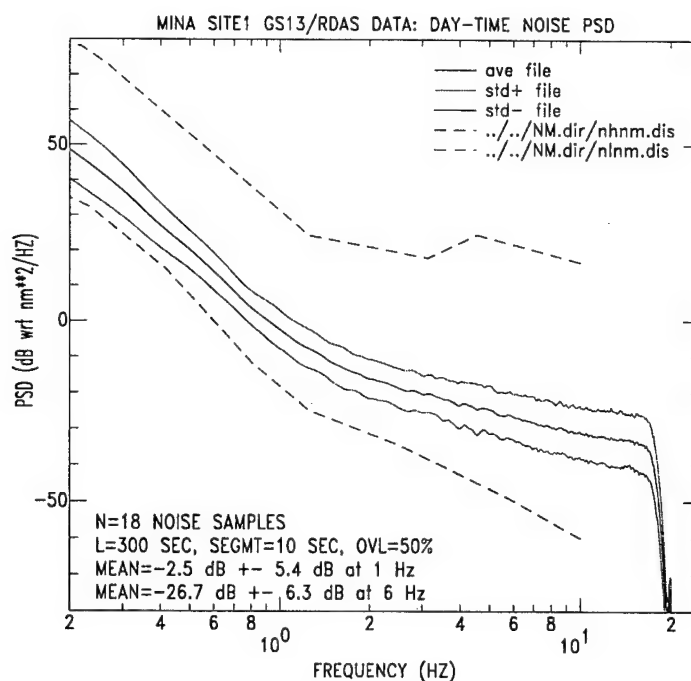


Figure A1. Daytime mean noise PSD at Mina Site 1. There are N=18 time series of noise samples. Each time series has a length L=300 seconds and is segmented by segments of SEGMENT=10 seconds. Segments were overlapped by OVL=50%.

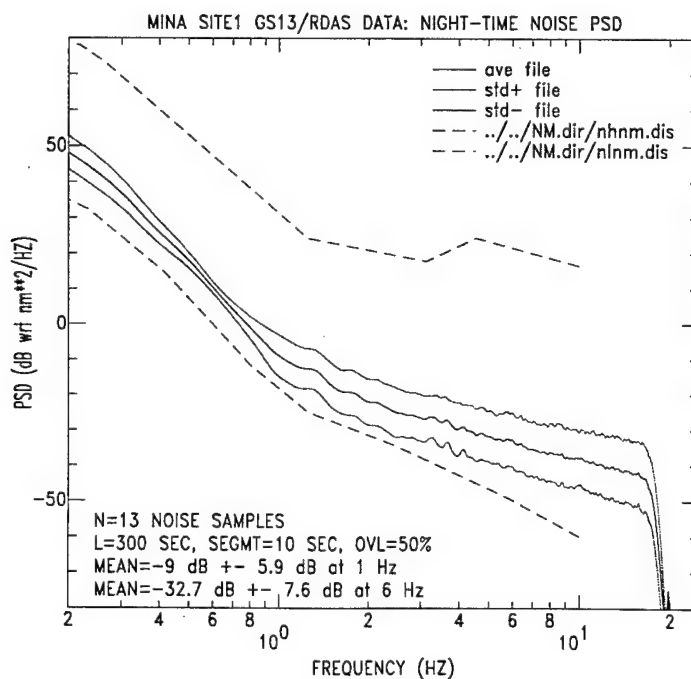


Figure A2. Nighttime mean noise PSD at Mina Site 1. There are N=13 time series of noise samples. Each time series has a length L=300 seconds and is segmented by segments of SEGMENT=10 seconds. Segments were overlapped by OVL=50%.

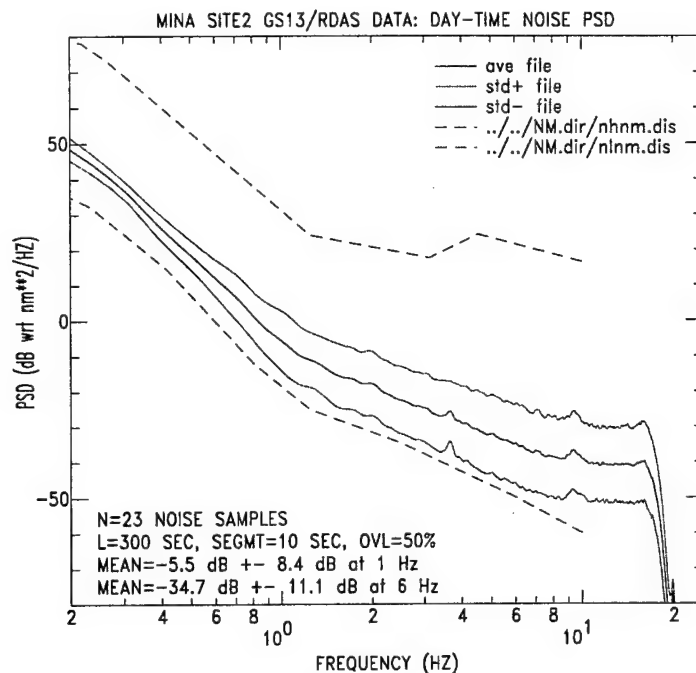


Figure A3. Daytime mean noise PSD at Mina Site 2. There are N=23 time series of noise samples. Each time series has a length L=300 seconds and is segmented by segments of SEGMENT=10 seconds. Segments were overlapped by OVL=50%.

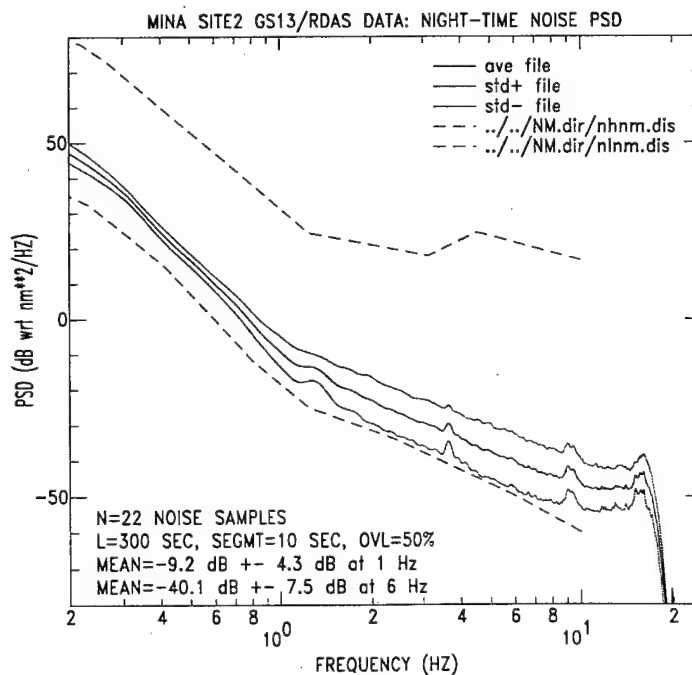


Figure A4. Nighttime mean noise PSD at Mina Site 2. There are N=22 time series of noise samples. Each time series has a length L=300 seconds and is segmented by segments of SEGMENT=10 seconds. Segments were overlapped by OVL=50%.

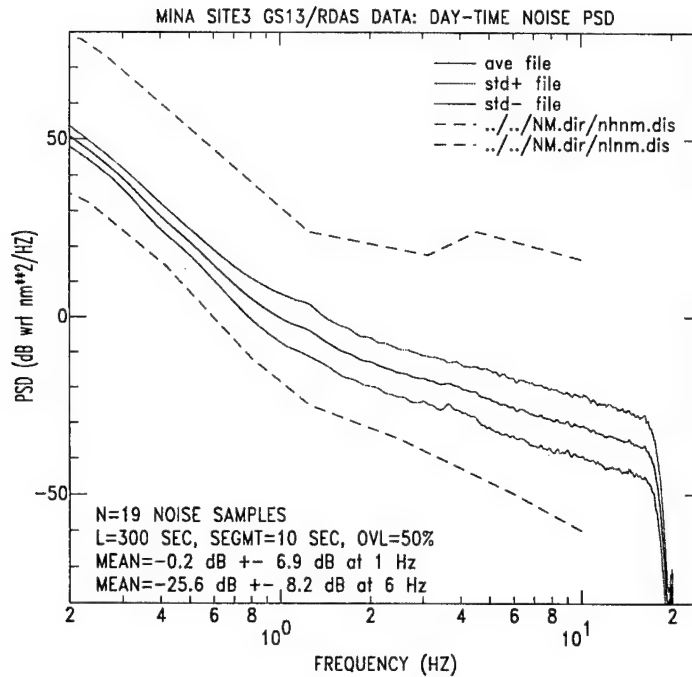


Figure A5. Daytime mean noise PSD at Mina Site 3. There are N=19 time series of noise samples. Each time series has a length L=300 seconds and is segmented by segments of SEGMENT=10 seconds. Segments were overlapped by OVL=50%.

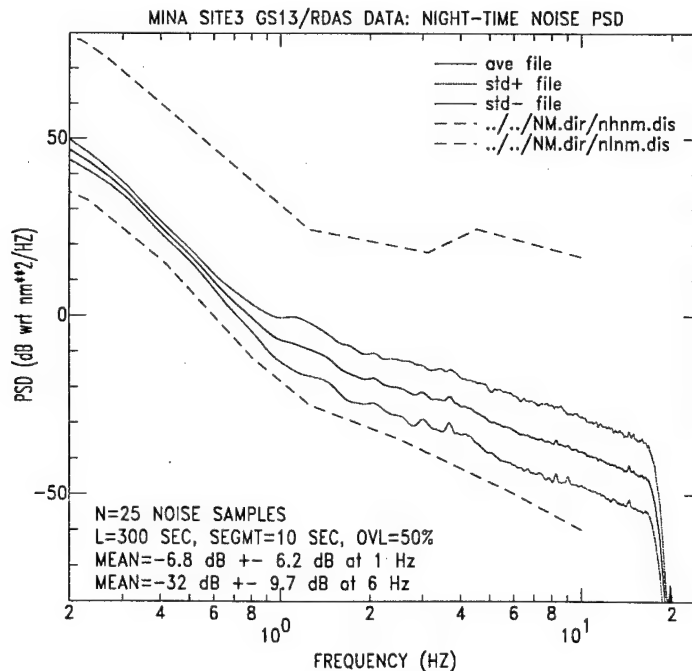


Figure A6. Nighttime mean noise PSD at Mina Site 3. There are N=25 time series of noise samples. Each time series has a length L=300 seconds and is segmented by segments of SEGMENT=10 seconds. Segments were overlapped by OVL=50%.

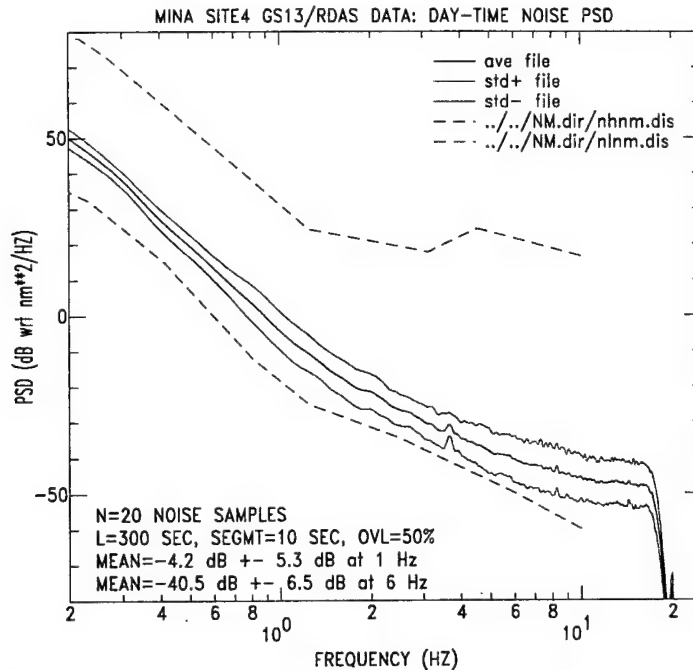


Figure A7. Daytime mean noise PSD at Mina Site 4. There are N=20 time series of noise samples. Each time series has a length L=300 seconds and is segmented by segments of SEGMENT=10 seconds. Segments were overlapped by OVL=50%.

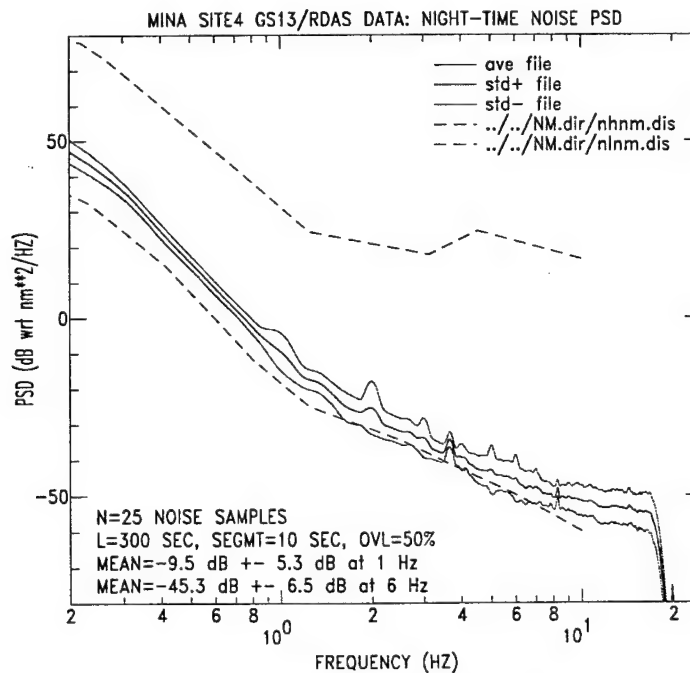


Figure A8. Nighttime mean noise PSD at Mina Site 4. There are N=25 time series of noise samples. Each time series has a length L=300 seconds and is segmented by segments of SEGMENT=10 seconds. Segments were overlapped by OVL=50%.

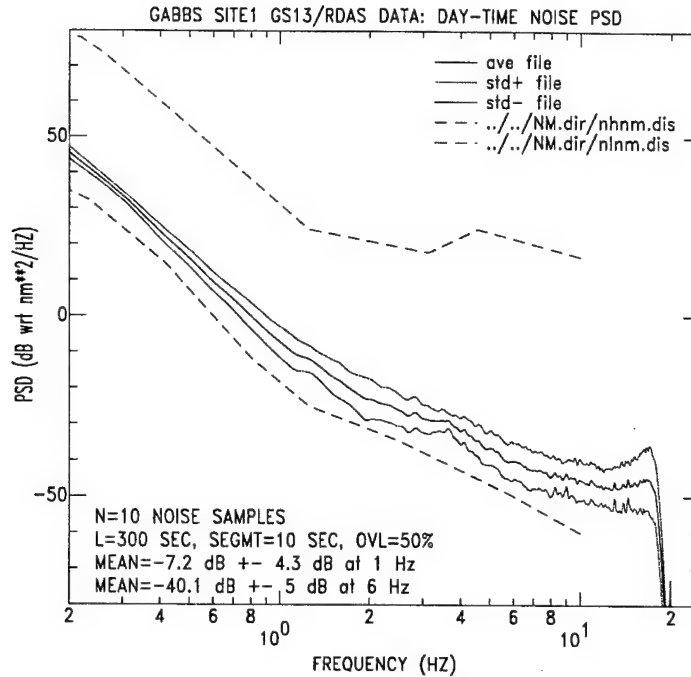


Figure A9. Daytime mean noise PSD at Gabbs Site 1. There are N=10 time series of noise samples. Each time series has a length L=300 seconds and is segmented by segments of SEGMENT=10 seconds. Segments were overlapped by OVL=50%.

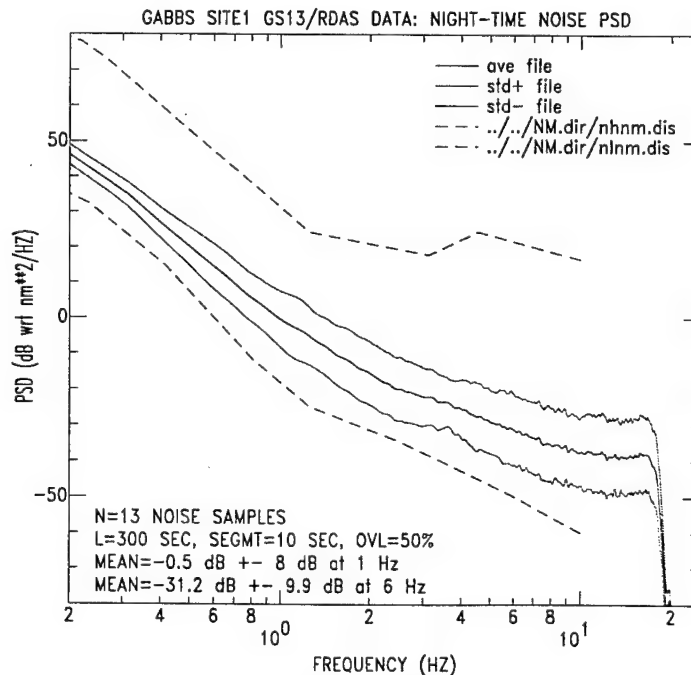


Figure A10. Nighttime mean noise PSD at Gabbs Site 1. There are N=13 time series of noise samples. Each time series has a length L=300 seconds and is segmented by segments of SEGMENT=10 seconds. Segments were overlapped by OVL=50%.

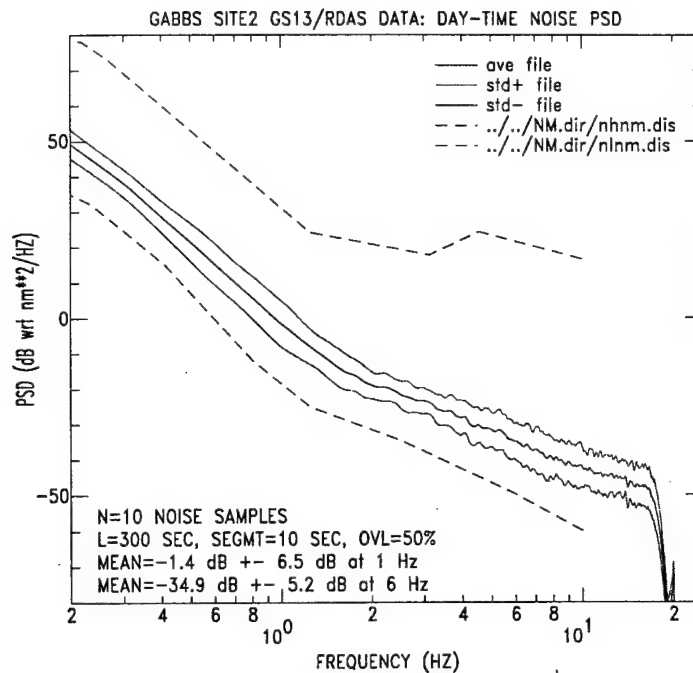


Figure A11. Daytime mean noise PSD at Gabbs Site 2. There are N=10 time series of noise samples. Each time series has a length L=300 seconds and is segmented by segments of SEGMT=10 seconds. Segments were overlapped by OVL=50%.

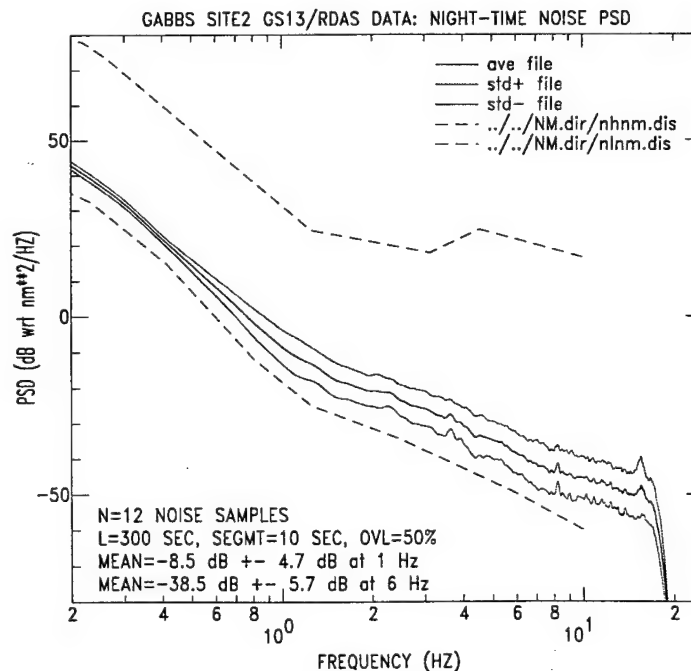


Figure A12. Nighttime mean noise PSD at Gabbs Site 2. There are N=12 time series of noise samples. Each time series has a length L=300 seconds and is segmented by segments of SEGMT=10 seconds. Segments were overlapped by OVL=50%.

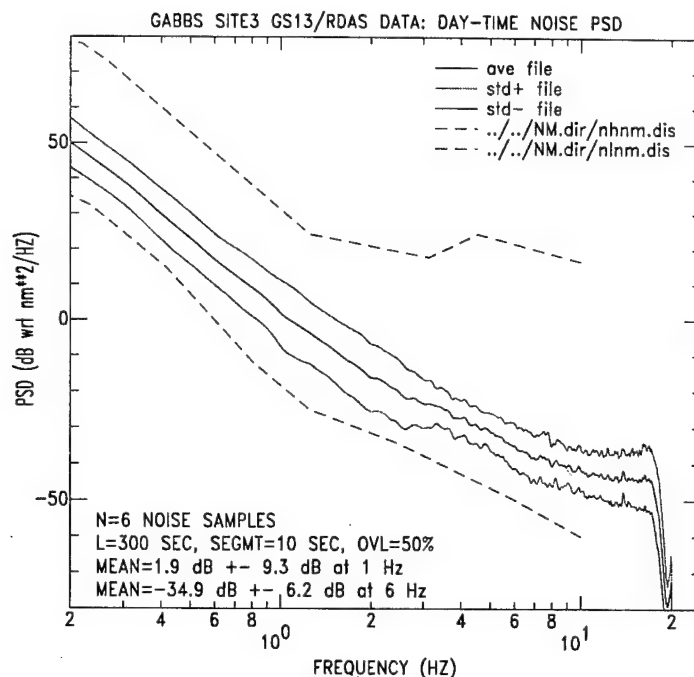


Figure A13. Daytime mean noise PSD at Gabbs Site 3. There are N=6 time series of noise samples. Each time series has a length L=300 seconds and is segmented by segments of SEGMENT=10 seconds. Segments were overlapped by OVL=50%.

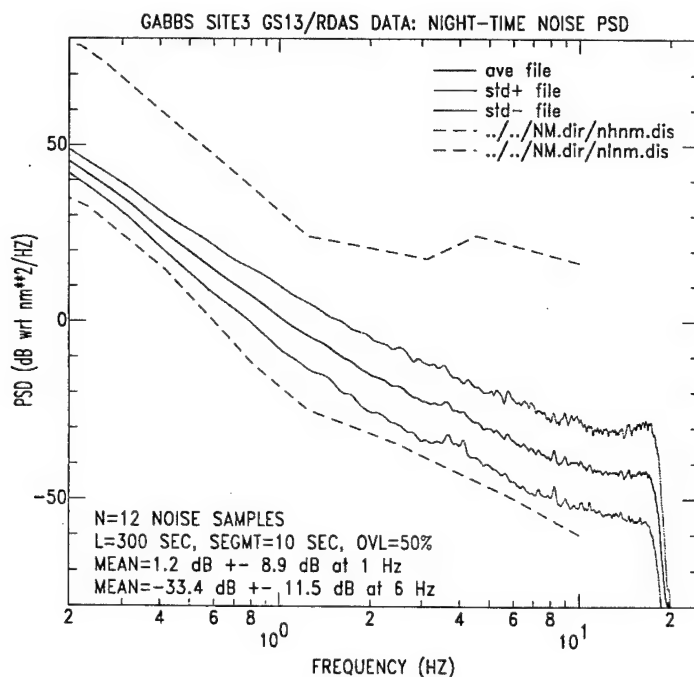


Figure A14. Nighttime mean noise PSD at Gabbs Site 3. There are N=12 time series of noise samples. Each time series has a length L=300 seconds and is segmented by segments of SEGMENT=10 seconds. Segments were overlapped by OVL=50%.

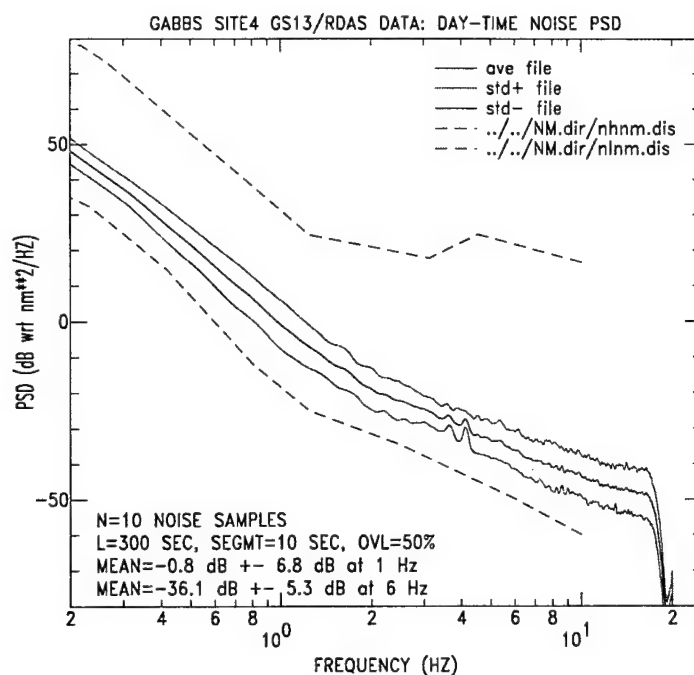


Figure A15. Daytime mean noise PSD at Gabbs Site 4. There are N=10 time series of noise samples. Each time series has a length L=300 seconds and is segmented by segments of SEGMT=10 seconds. Segments were overlapped by OVL=50%.

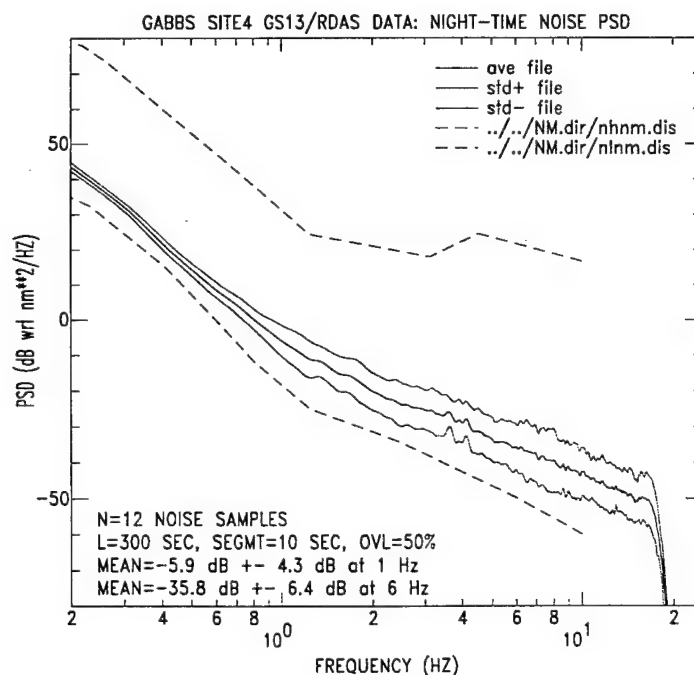


Figure A16. Nighttime mean noise PSD at Gabbs Site 4. There are N=12 time series of noise samples. Each time series has a length L=300 seconds and is segmented by segments of SEGMT=10 seconds. Segments were overlapped by OVL=50%.

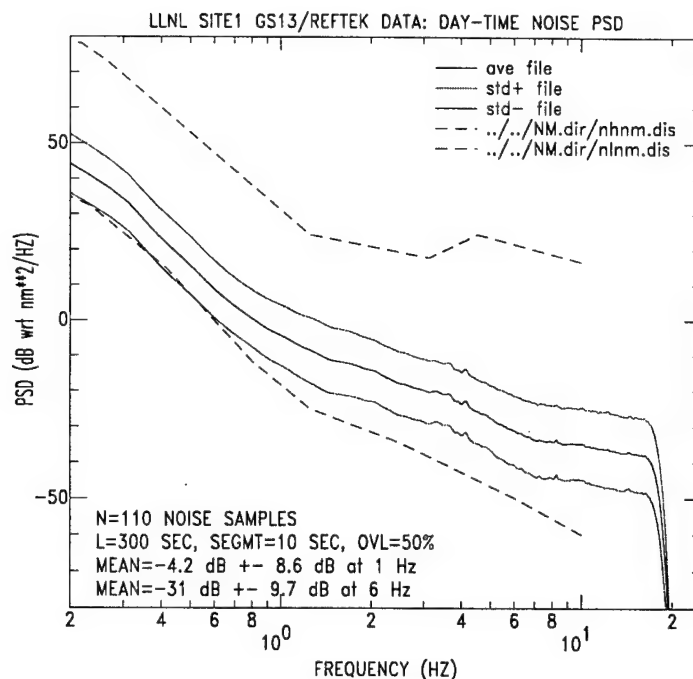


Figure A17. Daytime mean noise PSD at LLNL Site 1 (east of GAR). There are N=110 time series of noise samples. Each time series has a length L=300 seconds and is segmented by segments of SEGMENT=10 seconds. Segments were overlapped by OVL=50%.

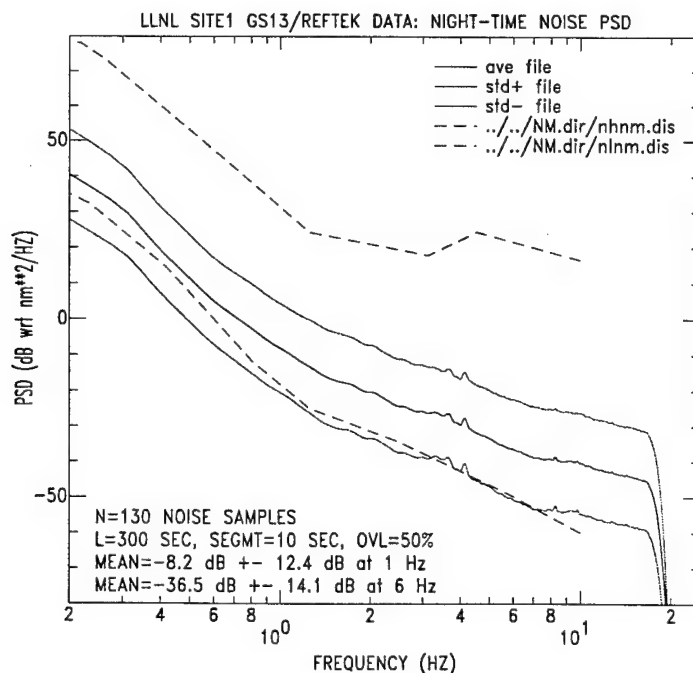


Figure A18. Nighttime mean noise PSD at LLNL Site 1 (east of GAR). There are N=130 time series of noise samples. Each time series has a length L=300 seconds and is segmented by segments of SEGMENT=10 seconds. Segments were overlapped by OVL=50%.

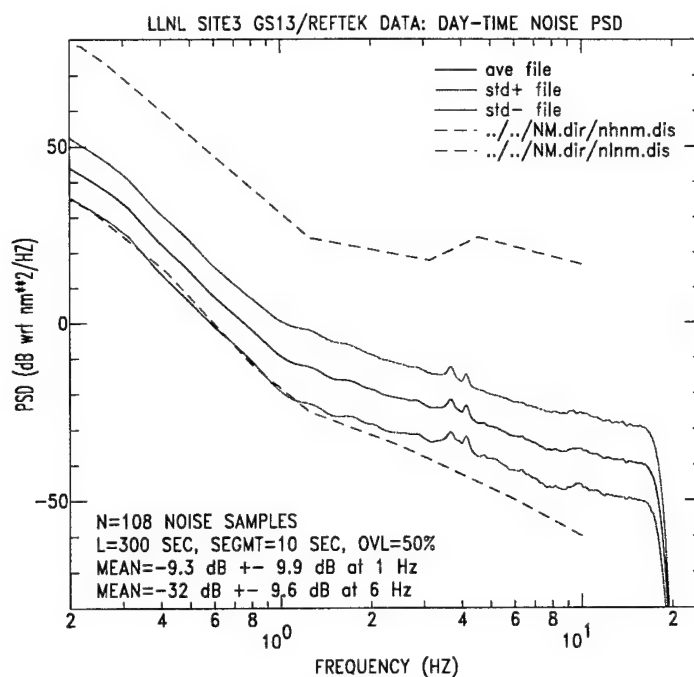


Figure A19. Daytime mean noise PSD at LLNL Site 3 (east of GAR). There are N=108 time series of noise samples. Each time series has a length L=300 seconds and is segmented by segments of SEGMT=10 seconds. Segments were overlapped by OVL=50%.

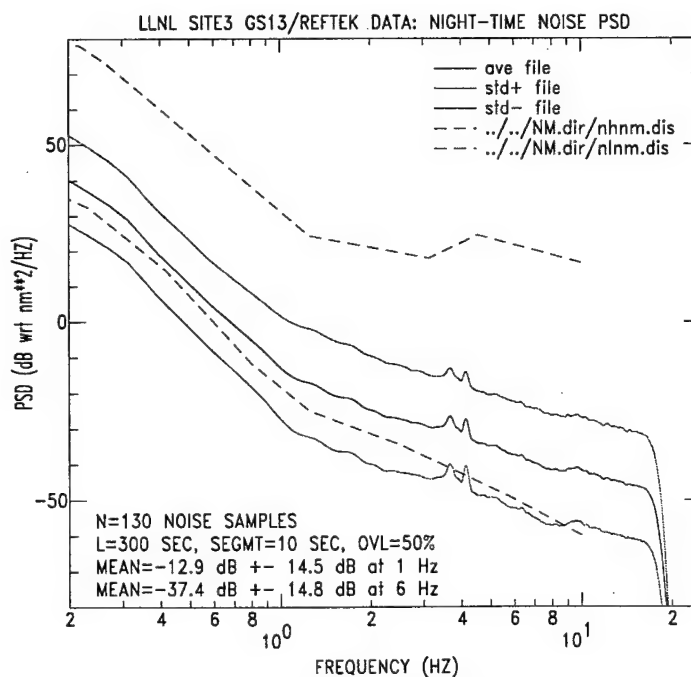


Figure A20. Nighttime mean noise PSD at LLNL Site 3 (east of GAR). There are N=130 time series of noise samples. Each time series has a length L=300 seconds and is segmented by segments of SEGMT=10 seconds. Segments were overlapped by OVL=50%.

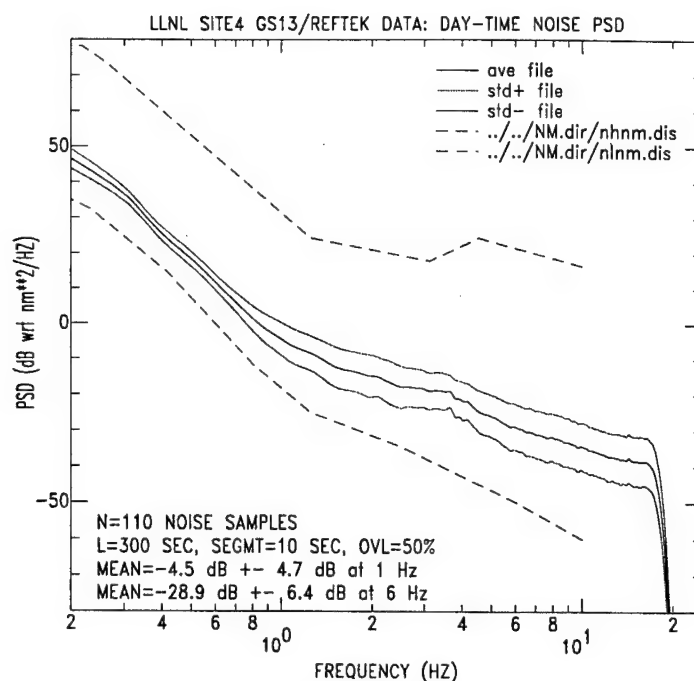


Figure A21. Daytime mean noise PSD at LLNL Site 4 (east of GAR). There are N=110 time series of noise samples. Each time series has a length L=300 seconds and is segmented by segments of SEGMENT=10 seconds. Segments were overlapped by OVL=50%.

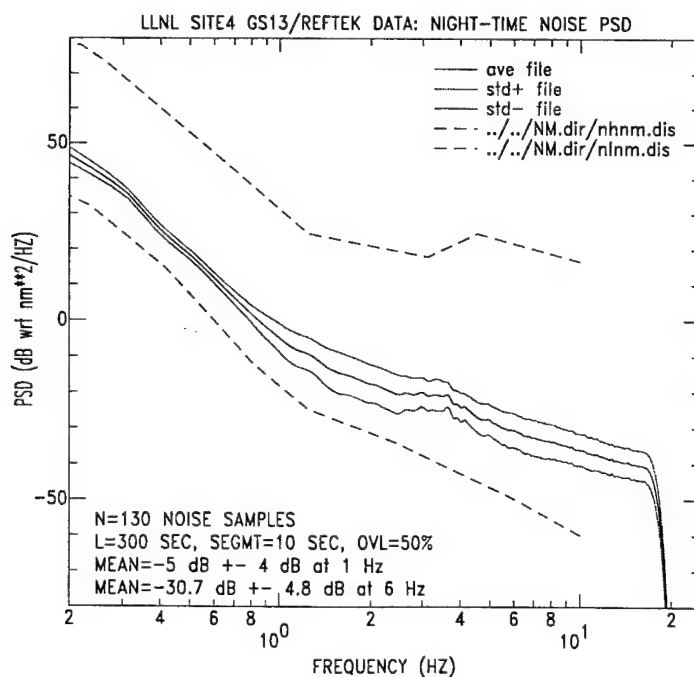


Figure A22. Nighttime mean noise PSD at LLNL Site 4 (east of GAR). There are N=130 time series of noise samples. Each time series has a length L=300 seconds and is segmented by segments of SEGMENT=10 seconds. Segments were overlapped by OVL=50%.

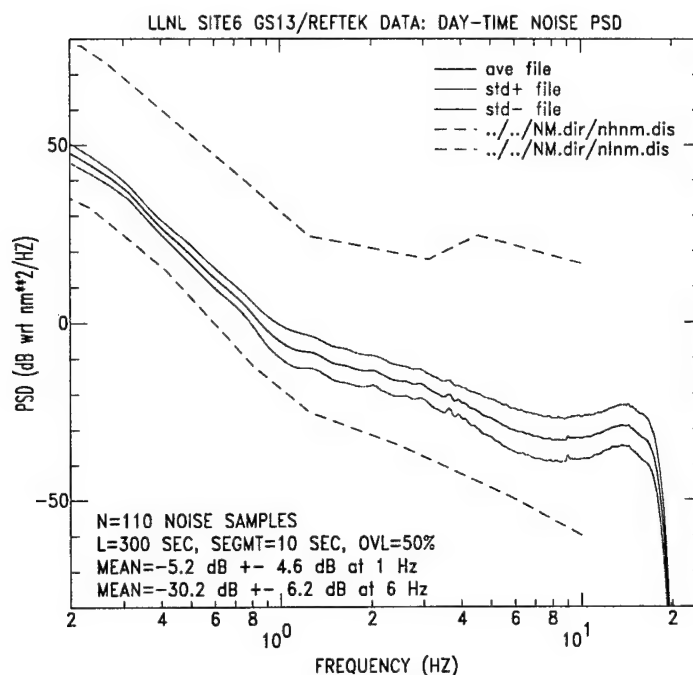


Figure A23. Daytime mean noise PSD at LLNL Site 6 (east of GAR). There are N=110 time series of noise samples. Each time series has a length L=300 seconds and is segmented by segments of SEGMENT=10 seconds. Segments were overlapped by OVL=50%.

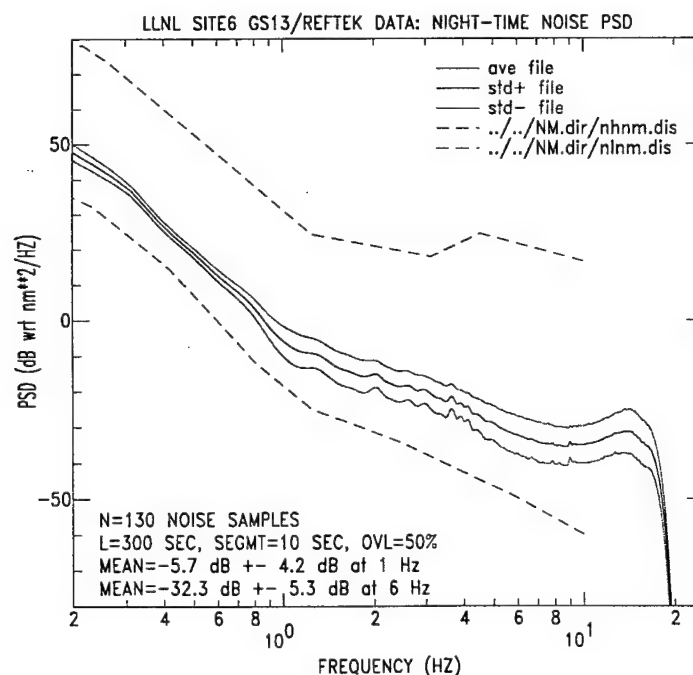


Figure A24. Nighttime mean noise PSD at LLNL Site 6 (east of GAR). There are N=130 time series of noise samples. Each time series has a length L=300 seconds and is segmented by segments of SEGMENT=10 seconds. Segments were overlapped by OVL=50%.

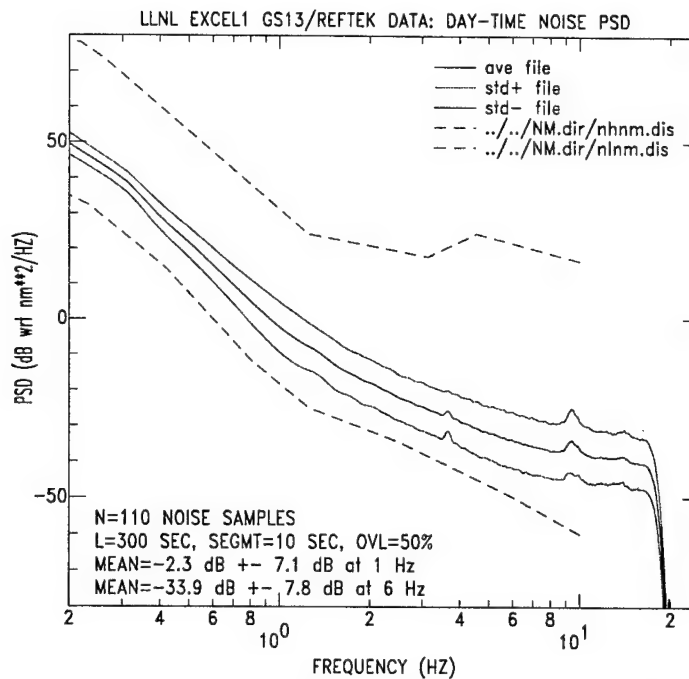


Figure A25. Daytime mean noise PSD at LLNL Excelsior Mountains Site 1. There are N=110 time series of noise samples. Each time series has a length L=300 seconds and is segmented by segments of SEGMT=10 seconds. Segments were overlapped by OVL=50%.

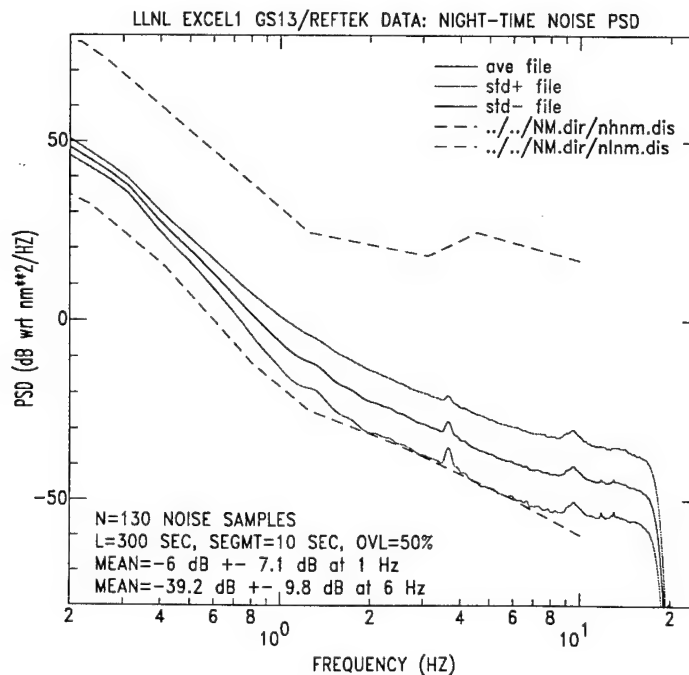


Figure A26. Nighttime mean noise PSD at LLNL Excelsior Mountains Site 1. There are N=130 time series of noise samples. Each time series has a length L=300 seconds and is segmented by segments of SEGMT=10 seconds. Segments were overlapped by OVL=50%.

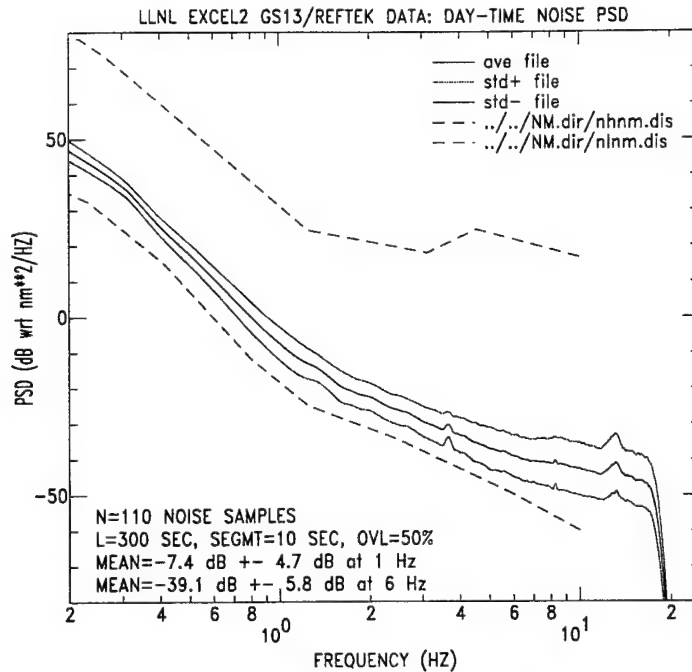


Figure A27. Daytime mean noise PSD at LLNL Excelsior Mountains Site 2. There are N=110 time series of noise samples. Each time series has a length L=300 seconds and is segmented by segments of SEGMENT=10 seconds. Segments were overlapped by OVL=50%.

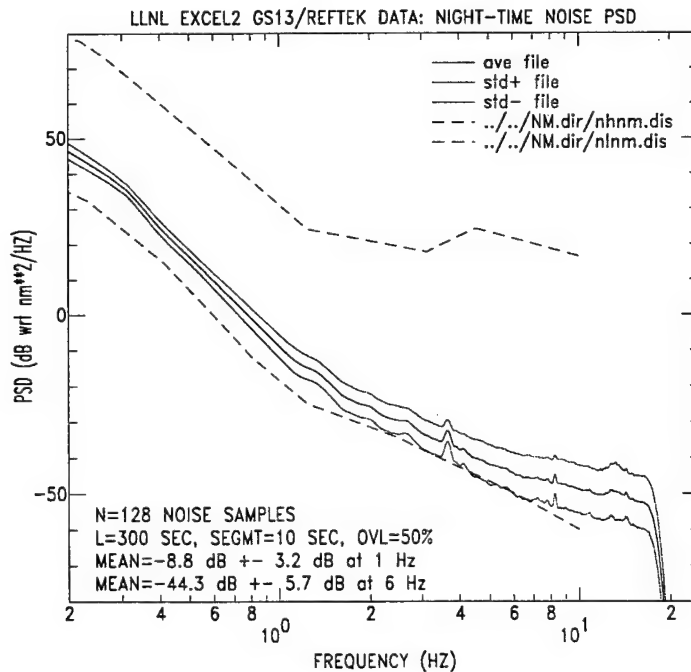


Figure A28. Nighttime mean noise PSD at LLNL Excelsior Mountains Site 2. There are N=128 time series of noise samples. Each time series has a length L=300 seconds and is segmented by segments of SEGMENT=10 seconds. Segments were overlapped by OVL=50%.

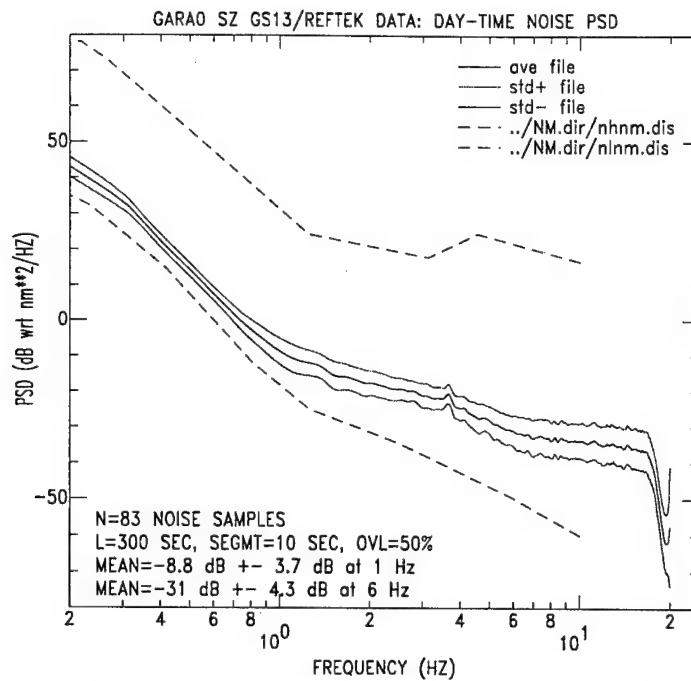


Figure A29. Daytime mean noise PSD at SMU GARA0 seismic station. There are N=83 time series of noise samples. Each time series has a length L=300 seconds and is segmented by segments of SEGMENT=10 seconds. Segments were overlapped by OVL=50%.

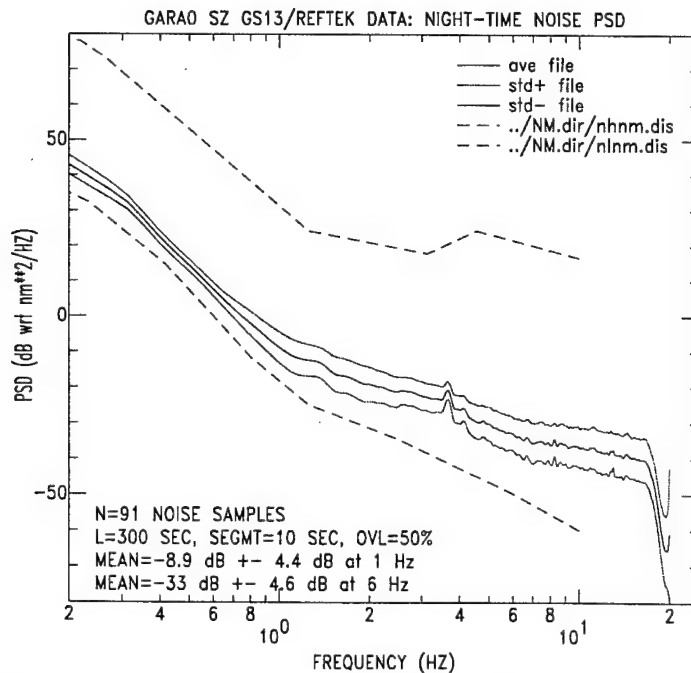


Figure A30. Nighttime mean noise PSD at SMU GARA0 seismic station. There are N=91 time series of noise samples. Each time series has a length L=300 seconds and is segmented by segments of SEGMENT=10 seconds. Segments were overlapped by OVL=50%.

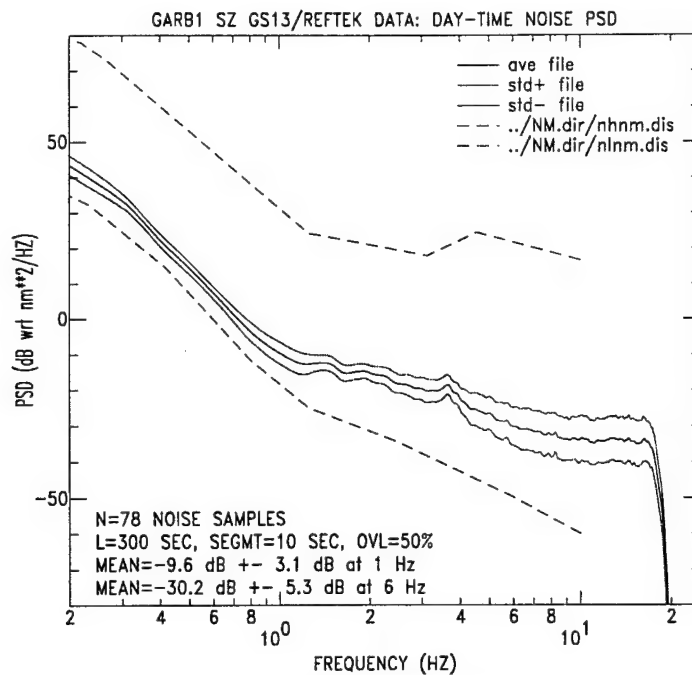


Figure A31. Daytime mean noise PSD at SMU GARB1 seismic station. There are N=78 time series of noise samples. Each time series has a length L=300 seconds and is segmented by segments of SEGMENT=10 seconds. Segments were overlapped by OVL=50%.

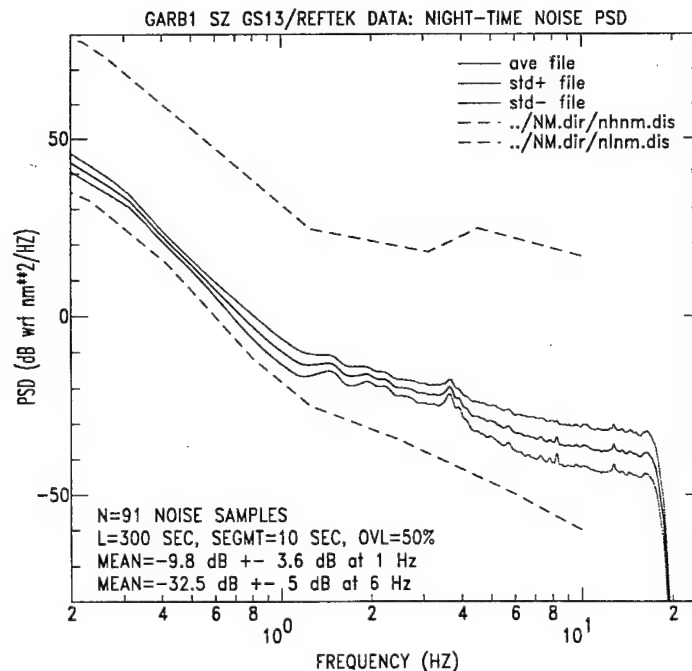


Figure A32. Nighttime mean noise PSD at SMU GARB1 seismic station. There are N=91 time series of noise samples. Each time series has a length L=300 seconds and is segmented by segments of SEGMENT=10 seconds. Segments were overlapped by OVL=50%.

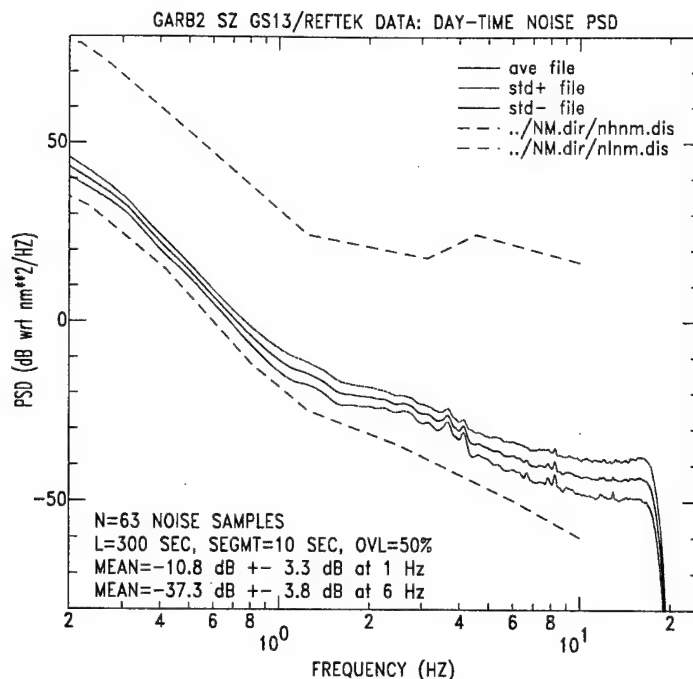


Figure A33. Daytime mean noise PSD at SMU GARB2 seismic station. There are N=69 time series of noise samples. Each time series has a length L=300 seconds and is segmented by segments of SEGMENT=10 seconds. Segments were overlapped by OVL=50%.

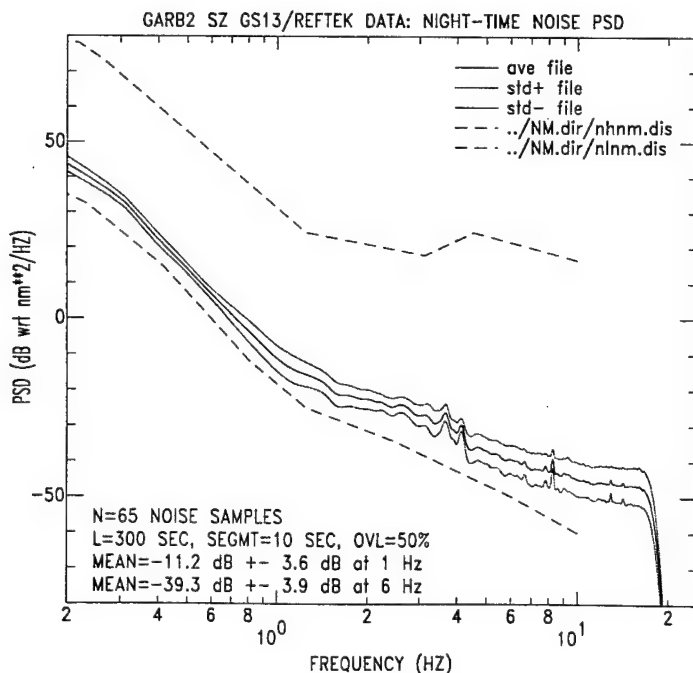


Figure A34. Nighttime mean noise PSD at SMU GARB2 seismic station. There are N=78 time series of noise samples. Each time series has a length L=300 seconds and is segmented by segments of SEGMENT=10 seconds. Segments were overlapped by OVL=50%.

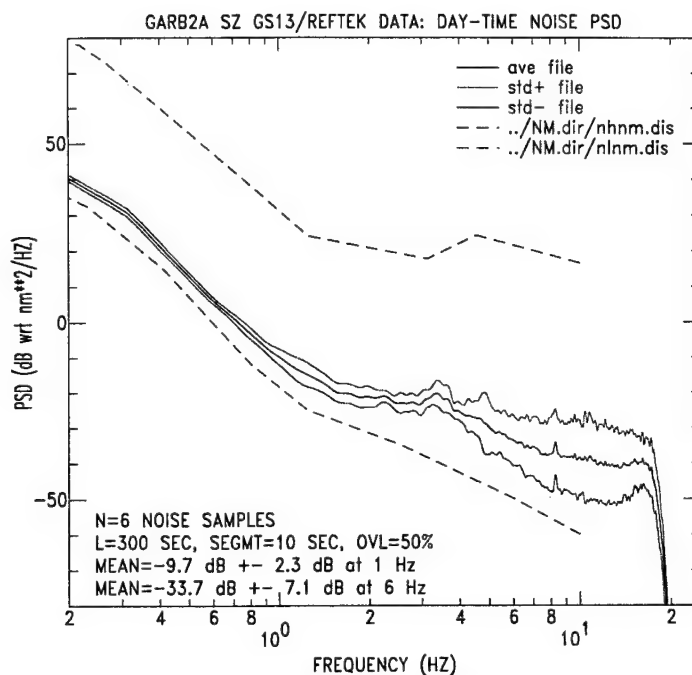


Figure A35. Daytime mean noise PSD at SMU GARB2A seismic station. There are N=6 time series of noise samples. Each time series has a length L=300 seconds and is segmented by segments of SEGMENT=10 seconds. Segments were overlapped by OVL=50%.

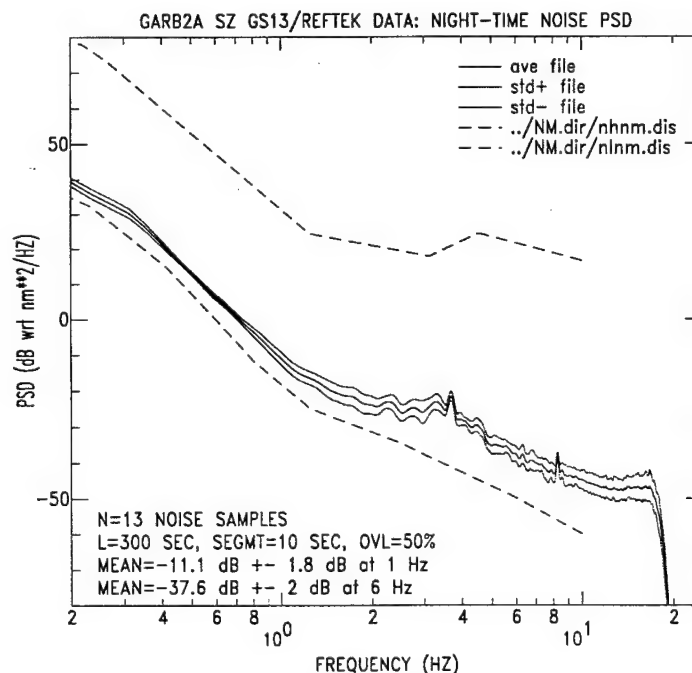


Figure A36. Nighttime mean noise PSD at SMU GARB2A seismic station. There are N=13 time series of noise samples. Each time series has a length L=300 seconds and is segmented by segments of SEGMENT=10 seconds. Segments were overlapped by OVL=50%.

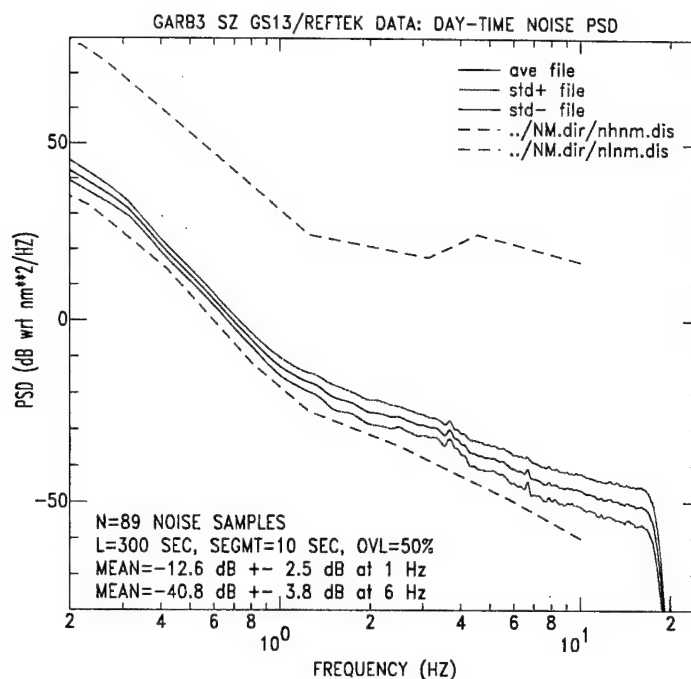


Figure A37. Daytime mean noise PSD at SMU GARB3 seismic station. There are N=89 time series of noise samples. Each time series has a length L=300 seconds and is segmented by segments of SEGMENT=10 seconds. Segments were overlapped by OVL=50%.

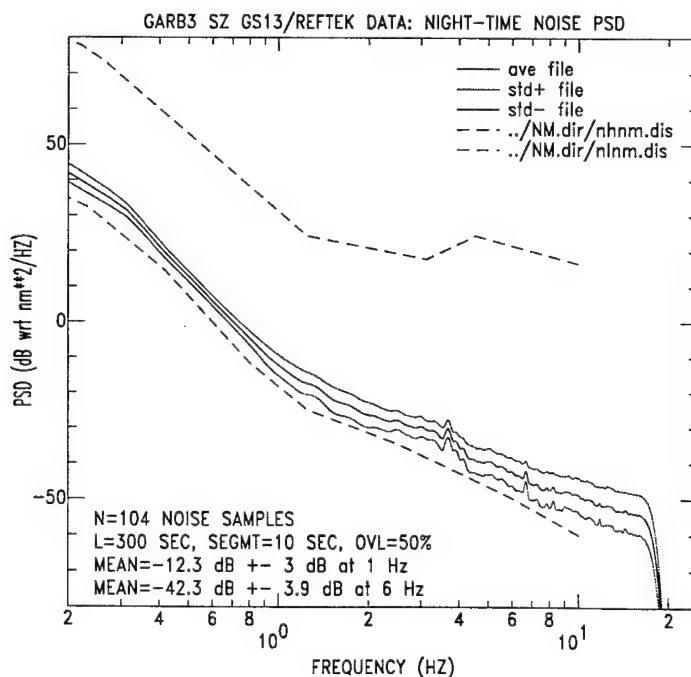


Figure A38. Nighttime mean noise PSD at SMU GARB3 seismic station. There are N=104 time series of noise samples. Each time series has a length L=300 seconds and is segmented by segments of SEGMENT=10 seconds. Segments were overlapped by OVL=50%.

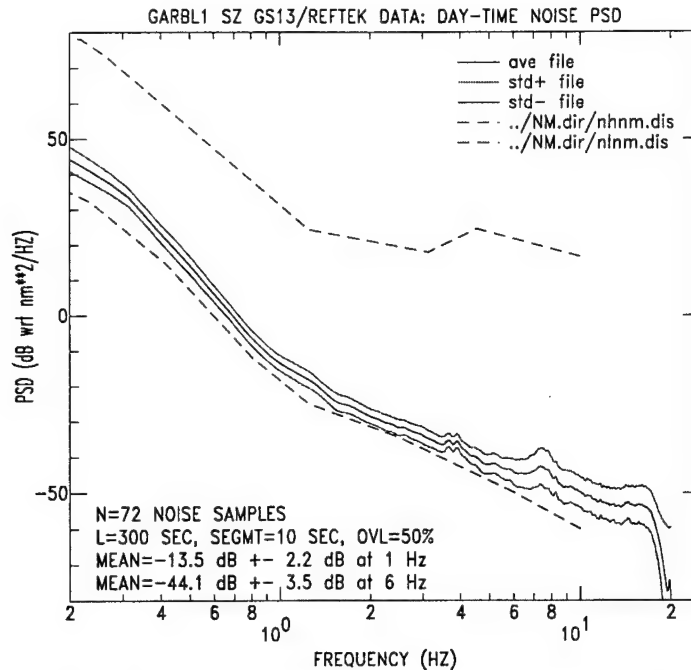


Figure A39. Daytime mean noise PSD at SMU GARBL1 seismic station. There are N=72 time series of noise samples. Each time series has a length L=300 seconds and is segmented by segments of SEGMENT=10 seconds. Segments were overlapped by OVL=50%.

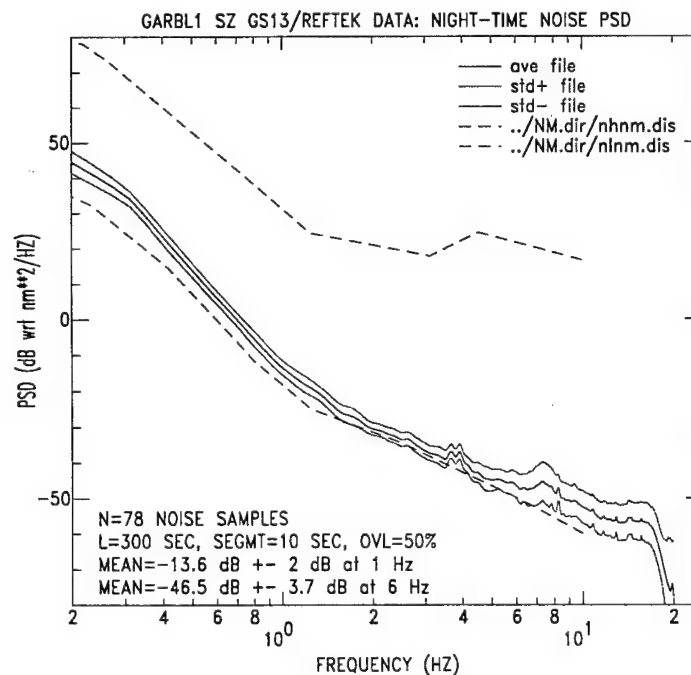


Figure A40. Nighttime mean noise PSD at SMU GARBL1 seismic station. There are N=78 time series of noise samples. Each time series has a length L=300 seconds and is segmented by segments of SEGMENT=10 seconds. Segments were overlapped by OVL=50%.

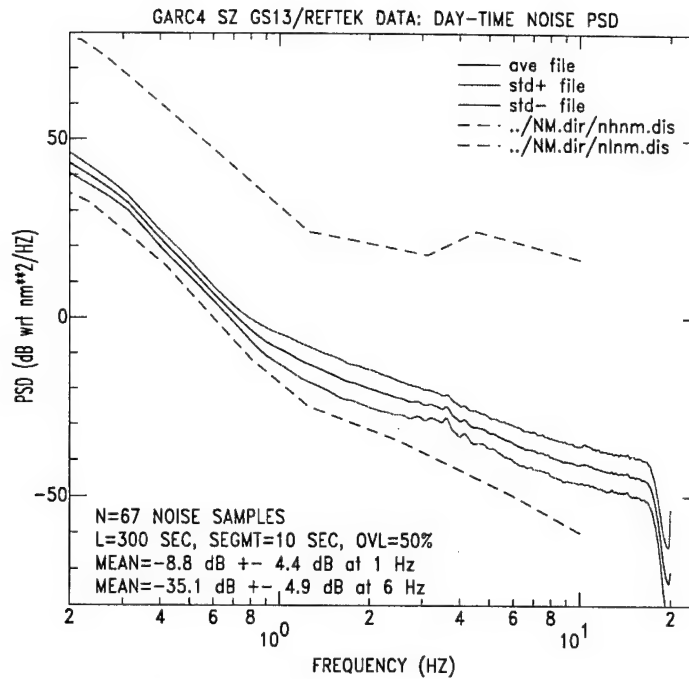


Figure A41. Daytime mean noise PSD at SMU GARC4 seismic station. There are N=67 time series of noise samples. Each time series has a length L=300 seconds and is segmented by segments of SEGMENT=10 seconds. Segments were overlapped by OVL=50%.

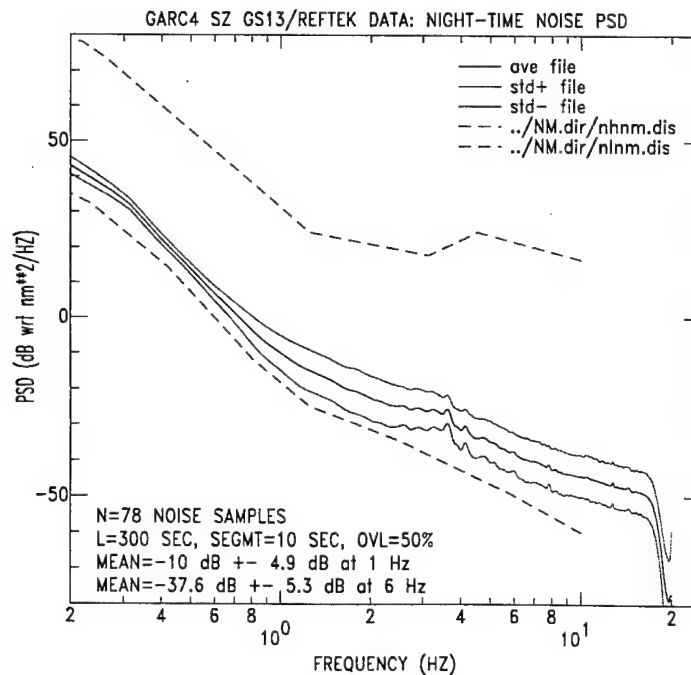


Figure A42. Nighttime mean noise PSD at SMU GARC4 seismic station. There are N=78 time series of noise samples. Each time series has a length L=300 seconds and is segmented by segments of SEGMENT=10 seconds. Segments were overlapped by OVL=50%.

APPENDIX B:
PLOTS OF SIGNAL AND NOISE COHERENCE SPECTRA

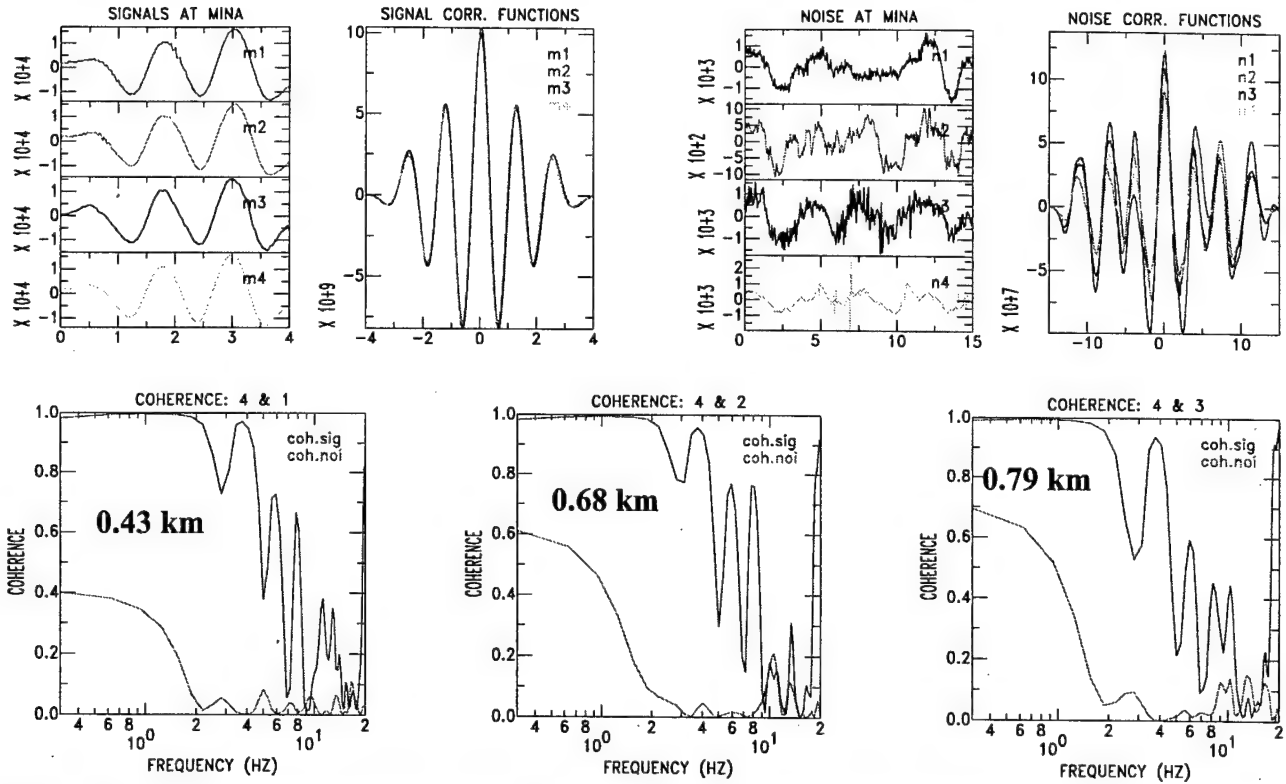


Figure B1. (a) Signals (P waves) recorded at MINA sites. (b) Signal correlation functions relative to site 4. (c) Pre-signal noise at four sites. (d) Noise correlation functions relative to site 4. (e-g) Signal and noise coherency of sites 1, 2, and 3, relative to site 4.

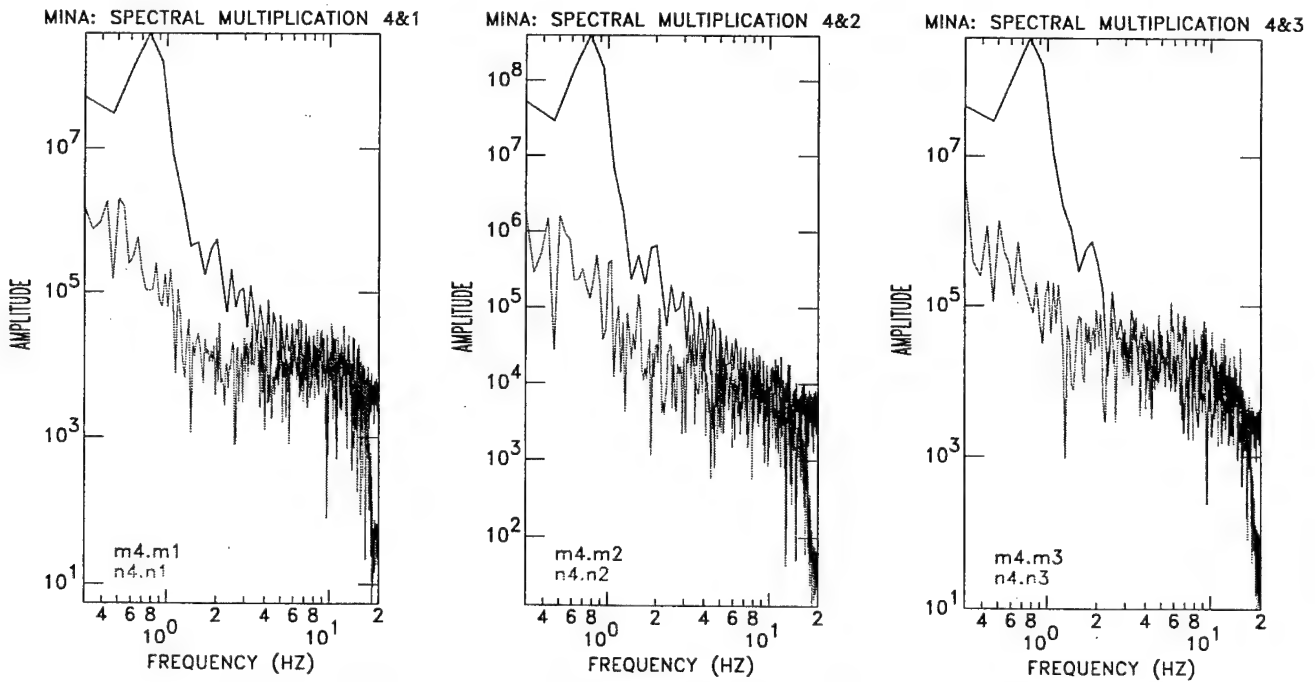


Figure B2. Spectral multiplications for signals as well as for pre-signal noise of sites 1, 2, and 3, with site 4.

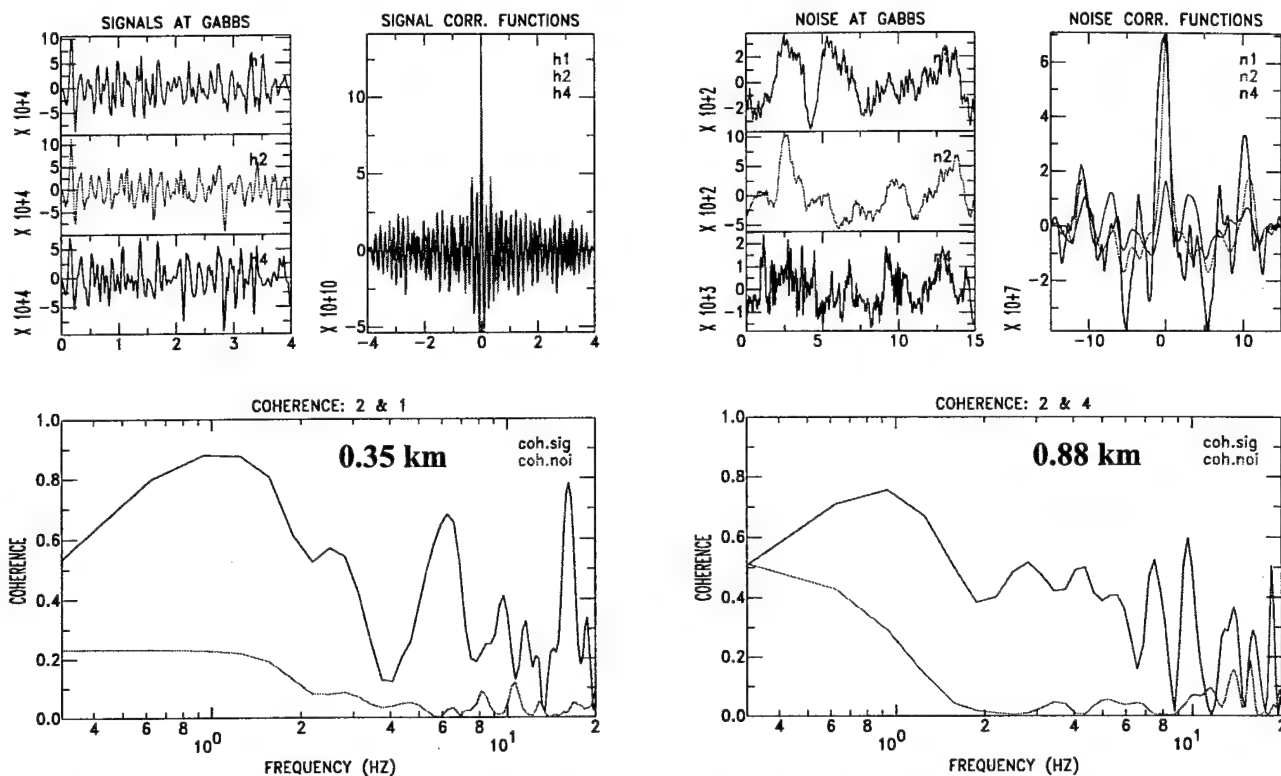


Figure B3. (a) Signals (P waves) recorded at GABBS sites. (b) Signal correlation functions relative to site 2. (c) Pre-signal noise at three sites. (d) Noise correlation functions relative to site 2. (e-f) Signal and noise coherency of sites 1 and 4, relative to site 2.

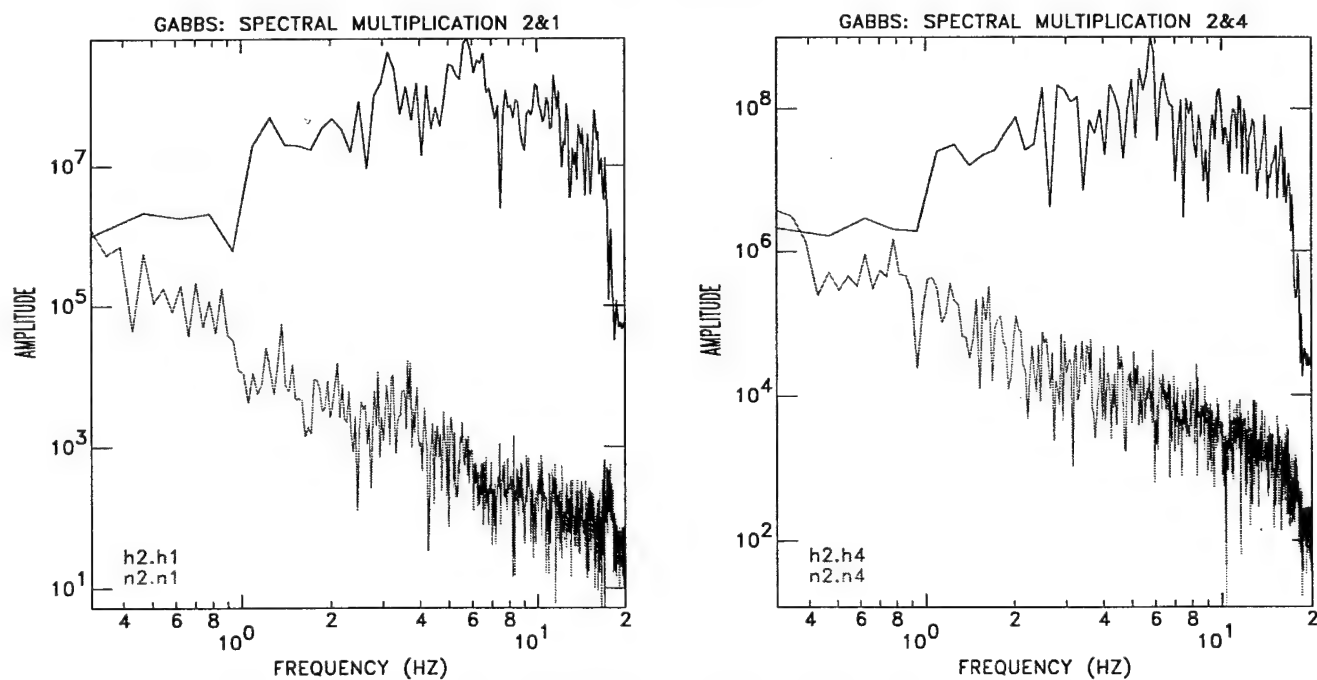


Figure B4. Spectral multiplications for signals as well as for pre-signal noise of sites 1 and 4, with site 2.

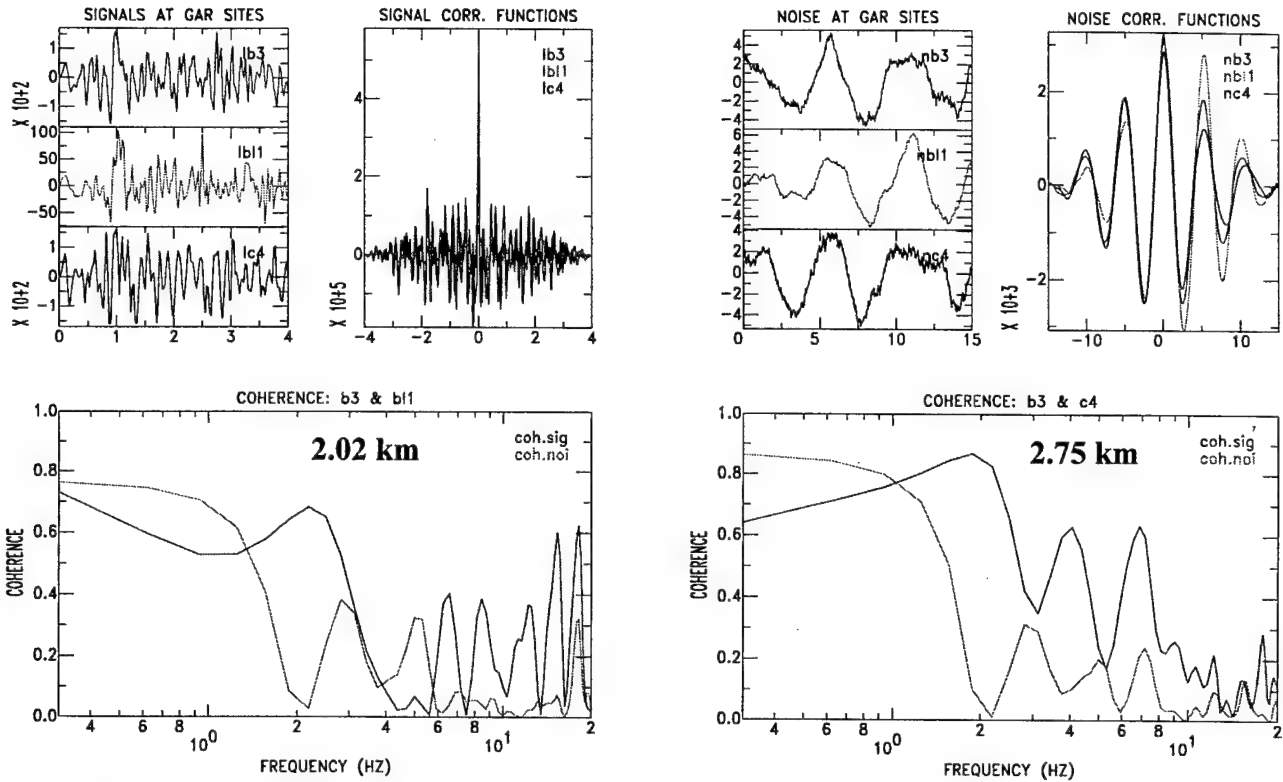


Figure B5. (a) Signals (P waves) recorded at GAR sites. (b) Signal correlation functions relative to site B3. (c) Pre-signal noise at three sites. (d) Noise correlation functions relative to site B3. (e-f) Signal and noise coherency of sites BL1 and C4, relative to site B3.

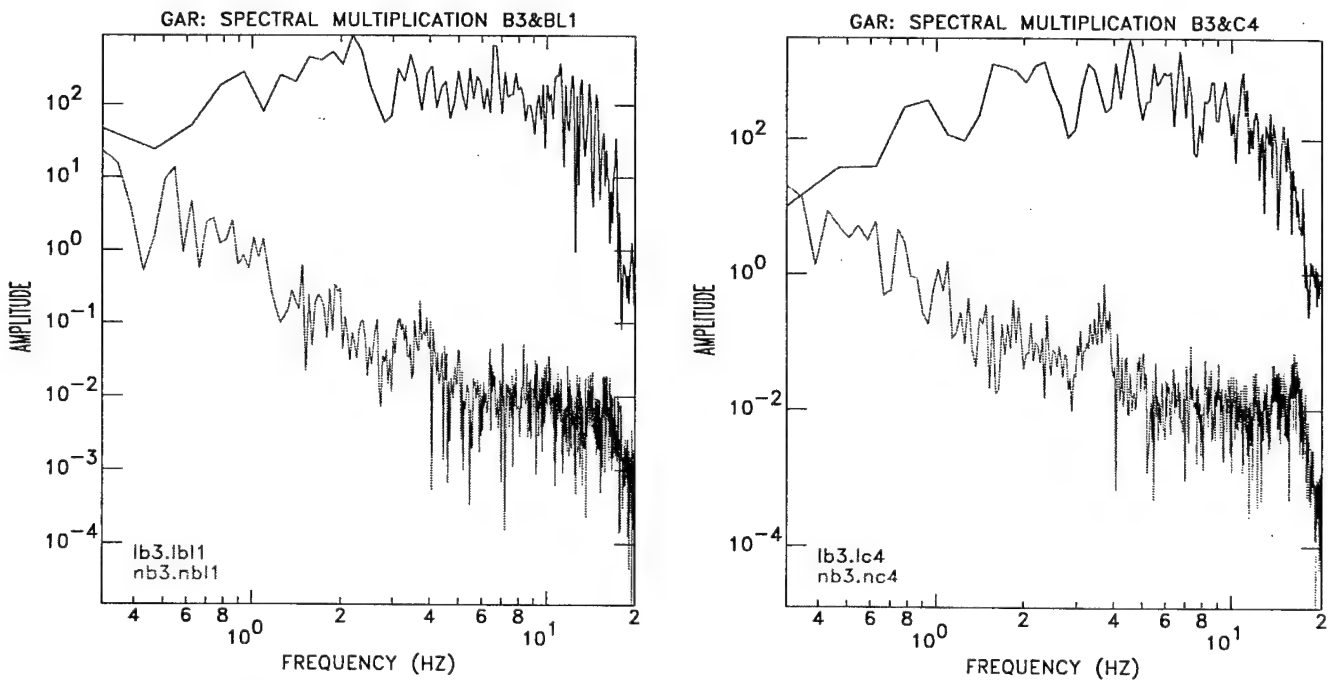


Figure B6. Spectral multiplications for signals as well as for pre-signal noise of sites BL1 and C4, with site B3.

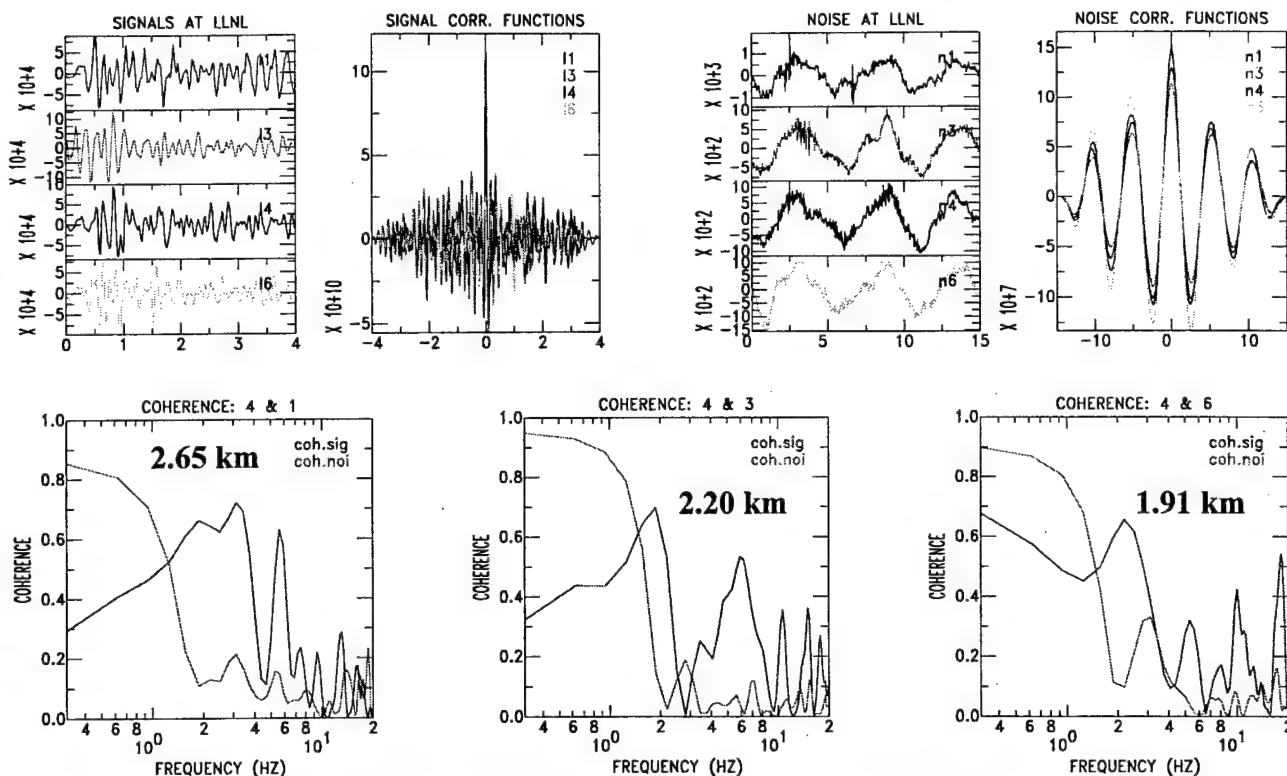


Figure B7. (a) Signals (P waves) recorded at LLNL sites. (b) Signal correlation functions relative to site 4. (c) Pre-signal noise at four sites. (d) Noise correlation functions relative to site 4. (e-g) Signal and noise coherency of sites 1, 3, and 6, relative to site 4.

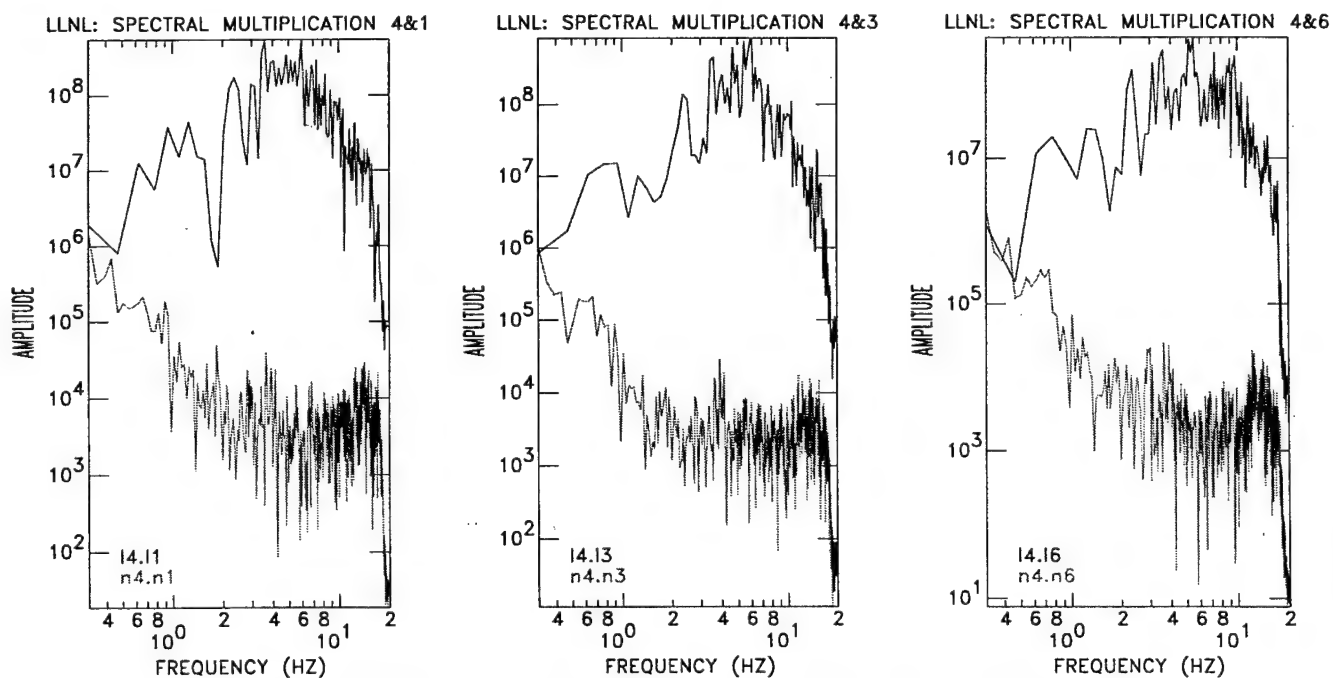


Figure B8. Spectral multiplications for signals as well as for pre-signal noise of sites 1, 3, and 6, with site 4.

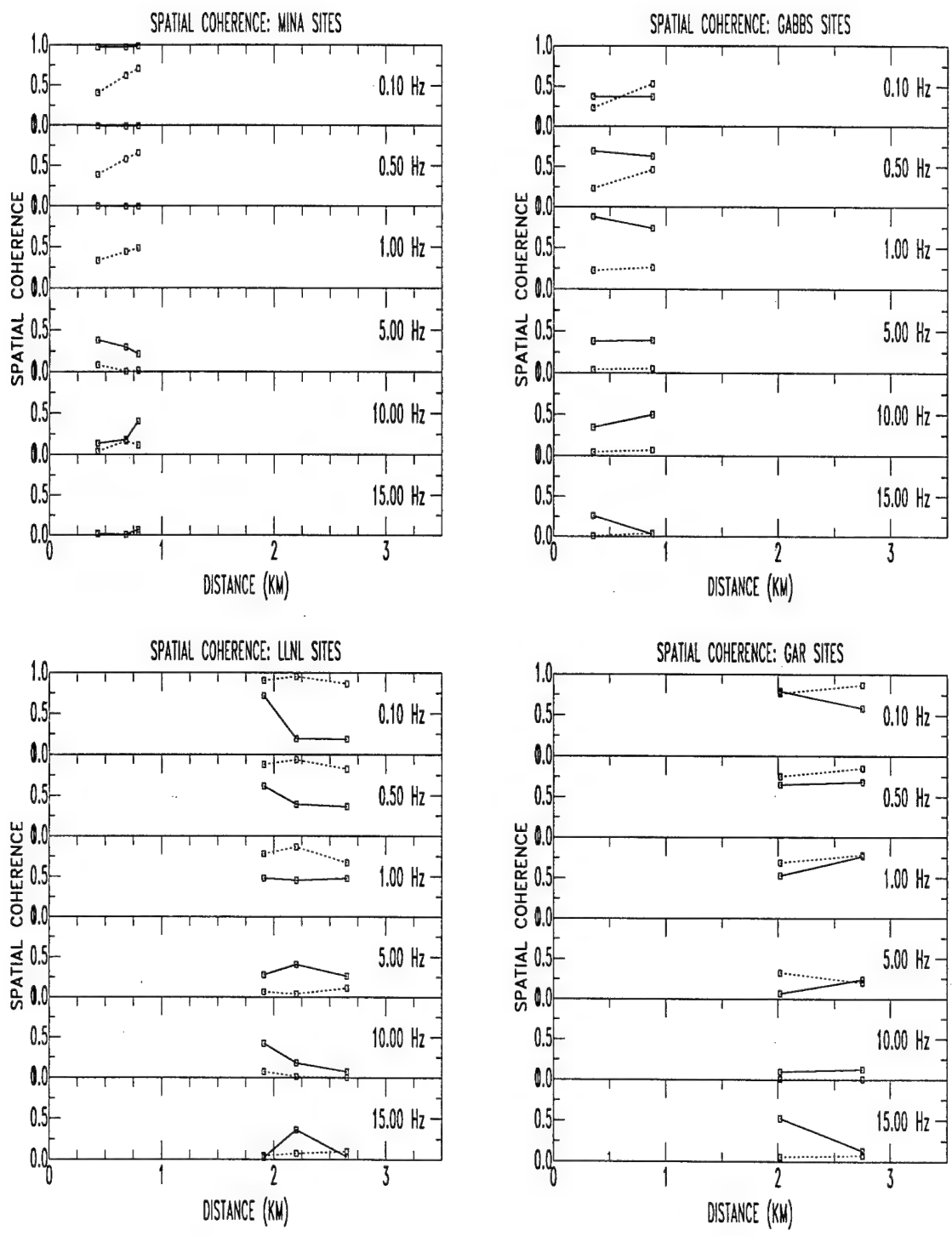


Figure B9. Spatial coherency as function of distance at some representative frequencies for signals (solid) and noise (dashed) at MINA, GABBS, LLNL, and GAR sites.

DISTRIBUTION

California Institute of Technology
ATTN: Prof. Thomas Ahrens
Seismological Laboratory, 252-21
Pasadena CA 91125

Air Force Research Laboratory
ATTN: Research Library/TL
5 Wright St.
Hanscom AFB MA 01731-3004

Air Force Research Laboratory
ATTN: VSOE
29 Randolph Rd.
Hanscom AFB MA 01731-3010

Air Force Research Laboratory
ATTN: AFRL/SUL
3550 Aberdeen Ave., SE
Kirtland AFB NM 87117-5776

NTPO
ATTN: Dr. R.W. Alewine
1901 N. Moore Street, Suite 609
Arlington VA 22209

Pennsylvania State University
ATTN: Prof. S. Alexander &
Prof. C.A. Langston
Department of Geosciences
537 Deike Building
University Park PA 16802

University of Colorado
ATTN: Prof. C. Archambeau, Prof. D. Harvey,
Dr. Anatoli Levshin, & Prof. M. Ritzwoller
Department of Physics
Campus Box 583
Boulder CO 80309-0583

Science Application International Corporation
ATTN: Dr. T. Bache, Jr. & Dr. T.J. Sereno
10260 Campus Point Drive
San Diego CA 92121-1578

Center for Monitoring Research
ATTN: Librarian
1300 N. 17th St., Suite 1450
Arlington VA 22209

Cornell University
ATTN: Prof. M. Barazangi
Institute for the Study of the Continents
Department of Geological Sciences
3126 SNEE Hall
Ithaca NY 14853

State University of New York, Binghamton
ATTN: Prof. F.T. Wu
Department of Geological Sciences
Binghamton NY 13901

Maxwell Technologies
ATTN: Dr. T.G. Barker & Dr. J. Stevens
8888 Balboa Ave.
San Diego CA 92123-1506

ENSCO, Inc./APA Division
ATTN: Dr. D.R. Baumgardt & Dr. Z. Der
5400 Port Royal Road
Springfield VA 22151-2388

University of Arizona
ATTN: Dr. S. Beck & Prof. T.C. Wallace
Department of Geosciences
Gould Simpson Building
Tuscon AZ 85721

Maxwell Technologies
ATTN: Dr. T.J. Bennett & Mr. J. Murphy
Geophysics & Resource Technologies Group
11800 Sunrise Valley Drive, Suite 1212
Reston VA 22091

University of California, San Diego
ATTN: Dr. J. Berger, Dr. L. Burdick, Dr. H.
Given, Dr. M. Hedlin, Prof. B. Minster,
Prof. J.A. Orcutt, & Dr. F.L. Vernon
Scripps Institution of Oceanography
IGPP, 0225
9500 Gilman Dr.
La Jolla CA 92093-0255

Schlumberger-Doll Research Center
ATTN: Dr. R. Burridge
Old Quarry Road
Ridgefield CT 06877

Department of Energy
ATTN: Ms. Leslie A. Casey
Office of R&D, NN-20
1000 Independence Ave., SW
Washington DC 20585-0420

Virginia Polytechnical Institute
ATTN: Dr. M. Chapman
Seismological Observatory
Department of Geological Sciences
4044 Derring Hall
Blacksburg VA 24061-0420

Arms Control & Disarmament Agency
ACDA/IVI/VC
ATTN: Mr. R. Cockerham & Mr. R. Morrow
320 21st Street N.W.
Washington DC 20451

University of Connecticut, Storrs
ATTN: Prof. V.F. Cormier
Department of Geology & Geophysics
U-45, Room 207
Storrs CT 06269-2045

HQ DSWA/PMA
ATTN: Dr. Anton Dainty
6801 Telegraph Rd.
Alexandria VA 22310-3398

San Diego State University
ATTN: Dr. S. Day
Department of Geological Sciences
San Diego CA 92182

Defense Technical Information Center
8725 John J. Kingman Road, Suite 0944
Ft. Belvoir VA 22060-6218

University of California, San Diego
ATTN: Dr. Catherine de Groot-Hedlin
Institute of Geophysics & Planetary Sciences
8604 La Jolla Shores Drive
San Diego CA 92093

University of Texas, El Paso
ATTN: Ms. Diane Doser
Department of Geological Sciences
El Paso TX 79968

Harvard University
ATTN: Prof. A. Dziewonski
Hoffman Laboratory
Department of Earth, Atmospheric &
Planetary Sciences
20 Oxford Street
Cambridge MA 02138

Boston College
ATTN: Prof. J. Ebel & Prof. A. Kafka
Department of Geology & Geophysics
Chestnut Hill MA 02167

Mission Research Corporation
ATTN: Dr. M. Fisk & Dr. W. Wortman
8560 Cinderbed Rd., Suite 700
Newington VA 22122

Brown University
ATTN: Prof. D. Forsyth
Department of Geological Sciences
Providence RI 02912

Defense Intelligence Agency/PAG-1A
ATTN: Dr. D.P. Glover
Washington DC 20340-6160

Multimax, Inc.
ATTN: Ms. Lori Grant
311C Forest Ave., Suite 3
Pacific Grove CA 93950

Southern Methodist University
ATTN: Dr. Henry Gray
Department of Statistics
P.O. Box 750302
Dallas TX 75275-0302

Multimax, Inc.
ATTN: Dr. I.N. Gupta & Mr. W. Rivers
1441 McCormick Drive
Largo MD 20774

Pacific Northwest National Laboratories
ATTN: Mr. D.N. Hagedorn
P.O. Box 999, MS F5-12
Richland WA 99352

Lawrence Livermore National Laboratory
ATTN: Dr. J. Hannon & Dr. K. Nakanishi
P.O. Box 808, L-205
Livermore CA 94550

MIT ERL E34-404
ATTN: Dr. David Harkrider
42 Carlton St.
Cambridge MA 02142-1324

New Mexico State University
ATTN: Prof. Thomas Hearn & Prof. James Ni
Department of Physics
Las Cruces NM 88003

California Institute of Technology
ATTN: Dr. Donald Helmberger
Division of Geological & Planetary Sciences
Seismological Laboratory
Pasadena CA 91125

Southern Methodist University
ATTN: Dr. E. Herrin & Dr. B. Stump
Department of Geological Sciences
P.O. Box 750395
Dallas TX 75275-0395

St. Louis University
ATTN: Prof. R. Herrmann & Prof. B. Mitchell
Department of Earth & Atmospheric Sciences
3507 Laclede Ave.
St. Louis MO 63103

HQ DSWA/PMP/CTBT
ATTN: Dr. M. Shore & Mr. Rong-Song Jih
6801 Telegraph Rd.
Alexandria VA 22310-3398

University of California, Berkeley
ATTN: Prof. L.R. Johnson &
Prof. T. McEvelly
Earth Sciences Division
LBNL 90-2106, MS 90-1116
479 McCone Hall
Berkeley CA 94720

Massachusetts Institute of Technology
ATTN: Prof. T.H. Jordan
Department of Earth, Atmospheric &
Planetary Sciences
77 Massachusetts Ave., 654-918
Cambridge MA 02139

Massachusetts Institute of Technology
ATTN: Dr. R. LaCross, M-200B
Lincoln Laboratory
P.O. Box 73
Lexington MA 02173-0073

University of Illinois, Urbana-Champaign
ATTN: Prof. F.K. Lamb & Prof. J. Sullivan
Department of Physics
1110 West Green Street
Urbana IL 61801

Oklahoma Geological Survey Observatory
ATTN: Dr. J. Lawson, Chief Geophysicist
P.O. Box 8
Leonard OK 74043-0008

University of California, Santa Cruz
ATTN: Dr. T. Lay, Dr. S. Schwartz, & Dr. R. Wu
Earth Sciences Dept.
Earth & Marine Sciences Building
Santa Cruz CA 95064

US Geological Survey
ATTN: Dr. W. Leith
920 National Center
Reston VA 22092

Weston Geophysical Corp.
ATTN: Mr. James Lewkowicz
325 West Main St.
Northboro MA 01532

ACDA/VI-OA
ATTN: Mr. A Lieberman
State Department Building, Room 5726
320 21st Street, NW
Washington DC 20451

AFTAC/CA(STINFO)/TT/TTR/TTD
1030 South Highway A1A
Patrick AFB FL 32925-3002

Georgia Institute of Technology
ATTN: Prof. L.T. Long
School of Geophysical Sciences
Atlanta G 30332

US Geological Survey
ATTN: Dr. R. Masse
Denver Federal Building
Box 25046, Mail Stop 907
Denver CO 80225

Southern Methodist University
ATTN: Dr. G. McCartor
Department of Physics
P.O. Box 750175
Dallas TX 75275-0175

US Geological Survey
ATTN: Dr. A. McGarr
National Earthquake Center
345 Middlefield Rd., MS-977
Menlo Park CA 94025

Center for Monitoring Research
ATTN: Dr. K.L. McLaughlin & Dr. R. North
1300 North 17th Street
Arlington VA 22209-3871

Office of the Secretary of Defense
DDR&E
Washington DC 20330

Yale University
ATTN: Prof. J. Park
Department of Geology & Geophysics
P.O. Box 208109
New Haven CT 06520-8109

University of Cambridge
ATTN: Prof. Keith Priestly
Bullard Labs, Department of Earth Sciences
Madingley Rise, Madingley Road
Cambridge CB3 0EZ, UNITED KINGDOM

BBN Systems & Technologies
ATTN: Dr. J.J. Pulli
1300 N. 17th St., Suite 1200
Arlington VA 22209

Defense Special Weapons Agency
ATTN: Dr. R. Reinke, FCDNA/FCTTS
1680 Texas S., SE
Kirtland AFB NM 87117-5669

DTR Associates
ATTN: Dr. Delaine Reiter
73 Standish Rd.
Watertown MA 02172

Columbia University
ATTN: Prof. P. Richards & Dr. J. Xie
Lamont-Doherty Geological Observatory
Route 9W
Palisades NY 10964

Woodward-Clyde Federal Services
ATTN: Dr. C.K. Saikia
566 El Dorado Street, Suite 100
Pasadena CA 91101-2560

University of Southern California, Los Angeles
ATTN: Prof. C.G. Sammis
Center for Earth Sciences
University Park
Los Angeles CA 90089-0741

Secretary of the Air Force
(SAFRD)
Washington DC 20330

University of California, Davis
ATTN: Dr. R. Shumway
Division of Statistics
410 MRAK Hall
Davis CA 95616-8671

AFOSR/NL
110 Duncan Avenue
Bolling AFB
Washington DC 20332-0001

Los Alamos National Laboratory
ATTN: Dr. H. Patton, Dr. S.R. Taylor,
Dr. Jill Warren, & Dr. T. Weaver
Geophysics Group EES-3, MS C335
P.O. Box 1663
Los Alamos NM 87545

Massachusetts Institute of Technology
ATTN: Prof. M.N. Toksoz
Earth Resources Lab, 34-440
42 Carleton Street
Cambridge MA 02142

ACIS
ATTN: Dr. L. Turnbull
New Headquarters Bldg., Room 4W03
Washington DC 20505

National Science Foundation
ATTN: Dr. Daniel Weill
Division of Earth Sciences, EAR-785
4201 Wilson Blvd., Room 785
Arlington VA 22230

I.R.I.G.M. - B.P. 68
ATTN: Dr. Michel Bouchon
38402 St. Martin D'Herès
Cedex, FRANCE

I.R.I.G.M. - B.P. 53
ATTN: Dr. Michel Campillo
Observatoire de Grenoble
38041 Grenoble, FRANCE

Ruhr University, Bochum
ATTN: Prof. Hans-Peter Harjes &
Dr. Johannes Schweitzer
Institute for Geophysics
P.O. Box 102148
W-4630 Bochum 1, GERMANY

NTNF/NORSAR
ATTN: Dr. Svein Mykkeltveit
P.O. Box 51
N-2007 Kjeller, NORWAY

Bureau of Mineral Resources
ATTN: Mr. David Jepsen, Acting Head,
Nuclear Monitoring Section
Geology and Geophysics
G.P.O. Box 378
Canberra, ACT 2601, AUSTRALIA

Atomic Weapons Establishment
ATTN: Dr. P. Marshall
Blacknest, Brimpton
Reading RG7 4RS, UNITED KINGDOM

Société Radiomana
ATTN: Dr. Bernard Massinon &
Dr. Pierre Mechler
27 rue Claude Bernard
75005 Paris, FRANCE

University of Bergen
ATTN: Prof. Eystein Husebye
Institute for Solid Earth Physics
Allegaten 40
N-5007, Bergen, NORWAY